

1 **Short title:** Integration of multi-omics data in potato

2
3 **Corresponding authors:** Kristina Gruden, kristina.gruden@nib.si; Markus Teige,
4 markus.teige@univie.ac.at
5

6 **Integration of multi-omics data and deep phenotyping provides insights**
7 **into responses to single and combined abiotic stress in potato**

8
9 Maja Zagorščak^{1*}, Lamis Abdelhakim^{2*}, Natalia Yaneth Rodriguez-Granados^{3*}, Jitka Široká^{4*},
10 Arindam Ghatak^{5*}, Carissa Bleker¹, Andrej Blejec¹, Jan Zrimec¹, Ondřej Novák⁴, Aleš Pěňčík⁴,
11 Špela Baebler¹, Lucia Perez Borroto⁶, Christian Schuy⁷, Anže Županič¹, Leila Afjehi-Sadat⁸,
12 Bernhard Wurzinger⁵, Wolfram Weckwerth^{5,9}, Maruša Pompe Novak^{1,10}, Marc R. Knight¹¹,
13 Miroslav Strnad⁴, Christian Bachem⁶, Palak Chaturvedi⁵, Sophia Sonnewald^{7†}, Rashmi
14 Sasidharan³⁺, Klára Panzarová²⁺, Kristina Gruden^{1+#}, Markus Teige^{5+#}

15
16 **Affiliations:**

17 ¹ Department of Biotechnology and Systems Biology, National Institute of Biology, Večna pot 121, 1000
18 Ljubljana, Slovenia

19 ² PSI (Photon Systems Instruments), spol. s r.o., Prumyslova 470, CZ-664 24 Drásov, Czech Republic

20 ³ Plant Stress Resilience, Institute of Environmental Biology, Utrecht University, Heidelberglaan 8, 3584
21 CS Utrecht, The Netherlands

22 ⁴ Laboratory of Growth Regulators, Palacký University in Olomouc & Institute of Experimental Botany AS
23 CR, Šlechtitelů 27, Olomouc, 779 00, Czech Republic

24 ⁵ Molecular Systems Biology (MOSYS), Department of Functional and Evolutionary Ecology, University
25 Vienna, Djerassiplatz 1, 1030 Vienna, Austria

26 ⁶ Wageningen University and Research, Plant Breeding, Droevendaalsesteeg 1, 6708 PB Wageningen,
27 The Netherlands

28 ⁷ Department Biologie, Lehrstuhl für Biochemie, Friedrich-Alexander-Universität Erlangen-Nürnberg,
29 Staudstr. 5, 91058 Erlangen, Germany

30 ⁸ Mass Spectrometry unit, Research Support Facilities, Faculty of Life Sciences, University Vienna,
31 Djerassiplatz 1, 1030 Vienna, Austria

32 ⁹ Vienna Metabolomics Center (VIME), University Vienna, Djerassiplatz 1, 1030 Vienna, Austria

33 ¹⁰ School for Viticulture and Enology, University of Nova Gorica, Gladni trg 8, 5271 Vipava, Slovenia

34 ¹¹ Department of Biosciences, Durham University, South Road, Durham DH1 3LE, United Kingdom

35
36 * shared first authorship

37 + shared last authorship

38 # corresponding authors

39
40 The authors responsible for distribution of materials integral to the findings presented in this
41 article in accordance with the policy described in the Instructions for Authors
42 (<https://academic.oup.com/plphys/pages/General-Instructions>) are Maja Zagorščak and Markus
43 Teige.

1 ABSTRACT

2 Potato (*Solanum tuberosum*) is highly water and space efficient but susceptible to abiotic stresses
3 such as heat, drought, and flooding, which are severely exacerbated by climate change. Our
4 understanding of crop acclimation to abiotic stress, however, remains limited. Here, we present a
5 comprehensive molecular and physiological high-throughput profiling of potato (*Solanum*
6 *tuberosum*, cv. Désirée) under heat, drought, and waterlogging applied as single stresses or in
7 combinations designed to mimic realistic future scenarios. Stress responses were monitored via
8 daily phenotyping and multi-omics analyses of leaf samples comprising proteomics, targeted
9 transcriptomics, metabolomics, and hormonomics at several timepoints during and after stress
10 treatments. Additionally, critical metabolites of tuber samples were analyzed at the end of the
11 stress period. We performed integrative multi-omics data analysis using a bioinformatic pipeline
12 that we established based on machine learning and knowledge networks. Waterlogging produced
13 the most immediate and dramatic effects on potato plants, interestingly activating ABA responses
14 similar to drought stress. In addition, we observed distinct stress signatures at multiple molecular
15 levels in response to heat or drought and to a combination of both. In response to all treatments,
16 we found a downregulation of photosynthesis at different molecular levels, an accumulation of
17 minor amino acids, and diverse stress-induced hormones. Our integrative multi-omics analysis
18 provides global insights into plant stress responses, facilitating improved breeding strategies
19 toward climate-adapted potato varieties.
20

21 **Keywords:** potato, *Solanum tuberosum*, abiotic stress responses, heat, drought, waterlogging,
22 multi-omics, integrative omics, adaptomics, panomics
23
24

25 INTRODUCTION

26 Improving crop resilience to climate change is a major challenge of modern agriculture (Bailey-
27 Serres et al., 2019; Rivero et al., 2022). High-yielding crop varieties including potato (*Solanum*
28 *tuberosum*), are vulnerable to heat, drought, and flooding (Benitez-Alfonso et al., 2023;
29 Zandalinas et al., 2023; Renziehausen et al., 2024; Sato et al., 2024). These environmental
30 stresses affect plant growth, source-sink relationships, sugar and hormone metabolism, among
31 other processes, which in turn, negatively impact product yield and nutritional status (Lal et al.,
32 2022). Potato is particularly sensitive to waterlogging (Jovović et al., 2021), and flooding of the
33 fields can ruin the entire harvest within a few days. Since global warming is increasing, the
34 occurrence of such extreme weather events, crop productivity worldwide is under considerable
35 threat (FAO, 2023). To ensure future food security, there is an urgent need for sustainable farming
36 practices including the development of stress tolerant varieties with consistent yields (Dahal et al.,
37 2019; Lal et al., 2022).
38

39 There is already a good understanding of how plants react to single abiotic stresses, which have
40 profound effects on plant metabolism and development. The primary effects of abiotic stress are

1 generation of reactive oxygen species (ROS), destabilization of proteins and changes in enzyme
2 efficiencies and membrane fluidity and integrity (Zhang et al., 2022). Together, these impacts
3 reduce plant productivity through changes in photosynthetic capacity, hormone balance, transport
4 of assimilates from source to sink as well as transport of soil nutrients and water by the roots. In
5 addition, species-specific vulnerabilities impact agronomic productivity, such as for instance tuber
6 initiation and tuber growth dynamics with potato. Potato tuber formation and growth is dependent
7 on mobile tuberization signals produced in source leaves, such as the potato homolog of
8 FLOWERING LOCUS T, SELF-PRUNING 6A (SP6A) (Navarro et al., 2011), that also regulates
9 directional transport of sucrose to the developing tuber (Abelenda et al., 2019). Heat, drought and
10 flooding trigger strong changes in gene expression and thereby strongly interfere with the
11 regulation of flowering and tuberization by the photoperiodic pathway. This leads to a delay in
12 tuberization and anomalies in subsequent tuber development such as second growth and/or
13 internal defects which together severely impacts marketable yields of the tuber crop (Dahal et al.,
14 2019; Lal et al., 2022).

15
16 On the other hand, the response of plants to combined stresses is unique and cannot be
17 extrapolated from the response to the corresponding individual stresses (Mittler, 2006).
18 Considering the increasing occurrences of simultaneous or sequential abiotic stresses in the field,
19 the relative lack of knowledge on multi-stress resilience is a major shortfall that hinders the ability
20 to develop effective strategies for crop improvement. Accordingly, the question of how
21 combinations of different stresses impact plants have recently gained a lot of interest (Zandalinas
22 et al., 2021). Several studies on combinatorial stress effects have been performed, especially
23 studying the physiological and molecular responses to combined heat- and drought stress in
24 potato (Demirel et al., 2020), wheat (Manjunath et al., 2023) and tomato (Zeng et al., 2024). In
25 nature, heat and drought often occur together, resulting in different physiological responses as
26 compared to individual stresses. For example, under heat stomatal conductance and transpiration
27 are increased to reduce leaf temperature, whilst under drought, stomata are closed to avoid water
28 loss, which leads to a strongly reduced CO₂-assimilation (Zhang and Sonnewald, 2017). The final
29 phenotypic output in a combined stress scenario greatly depends on synergistic and antagonistic
30 interactions between stress-specific signalling and response pathways. These interactions can
31 be regulated at various levels (gene expression to metabolism), and on different scales (cell to
32 system), thus resulting in complex regulatory network perturbations. Therefore, as information
33 gained by extrapolating from studies on individual stressors is limited, it is crucial to increase our
34 understanding of crop responses in multi-stress situations.

1
2 To this end, high-throughput phenotyping (HTP) platforms and integrative omics technologies can
3 measure molecular mechanisms at multiple levels and in multiple processes simultaneously. This
4 can help us obtain a comprehensive understanding of the intricate dynamics of plant-environment
5 interactions (Yang et al., 2020; Hall et al., 2022; Zhang et al., 2022). Here, advanced data
6 integration pipelines can aid with unbiased integration and systematic extraction of biological
7 knowledge from large multi-omics datasets (Cembrowska-Lech et al., 2023). However, despite
8 the increasing application of high-throughput approaches in agricultural and plant research, only
9 a handful of studies have addressed the problem of data integration from comprehensive multi-
10 omics data (Jamil et al., 2020). Therefore, to enable molecular insights across various system
11 levels and disentangle the intricate physiological and molecular crosstalk in the context of non-
12 additive effects of different stress combinations, it is imperative to develop and apply multi-omics
13 integrative approaches that leverage statistics, machine learning, and graph theory.

14
15 In this study, we aimed to increase knowledge on multiple abiotic stress responses of potato
16 plants and to integrate this into a complex knowledge network. Therefore, a comprehensive
17 assessment of potato responses to single and combined heat, drought, and waterlogging stress
18 was performed. Using the cv. Désirée, a widely used moderately stress-resistant potato cultivar,
19 we monitored dynamic changes in morphological, physiological as well as biochemical and
20 molecular responses under stress conditions. With the application of HTP, multi-omics
21 technologies, prior knowledge and multi-level integration approaches, we identified important
22 molecular signatures, unique to single and different stress combinations. These results can guide
23 the development of diagnostic markers for rapid detection of stress, allowing for earlier agricultural
24 interventions to enhance plant resilience towards abiotic stress and development of marker-
25 assisted breeding programs for climate-resilient crops (Weckwerth et al., 2020; Mishra et al.,
26 2024).

27 RESULTS

28 This study aims to increase the mechanistic understanding of potato acclimation to individual and
29 combined abiotic stresses. We focused on individual heat, drought, and waterlogging stresses,
30 as well as realistic combinations of these. We used the cv. Désirée, a widely used moderately
31 stress-resistant potato cultivar, as our model. To provide insights into multi-level regulation of

1 stress responses, we conducted HTP and comprehensive omics analyses, according to the
2 scheme outlined in Figure 1A (for more details, see Supp. Table S1).

3 Effects of single and combined stresses on potato growth and morphology

4
5 To assess potato phenotypic responses to different stress conditions, multiple morphological and
6 physiological traits (Supp. Table S2) were quantified daily, using several imaging sensors (Figure
7 1B). Using RGB side and top view imaging, we monitored changes in plant growth dynamics
8 during the stress treatments and recovery phases, considering traits such as plant volume, area,
9 height and compactness. We observed that all stress treatments negatively affected plant growth,
10 however, to different degrees (Figure 1C, Supp. Figure S1). Although individual drought (D, 30%
11 of field capacity) and heat stress (H, 30°C during the day, 28°C at night) decreased the rate of
12 biomass accumulation (plant volume, area, and height), we saw that heat had stronger effects
13 over time (Figure 1C, Supp. Figure S1A-C). The negative effects of heat became more severe
14 when combined with drought (HD, water withdrawal starting after 7 days of H) (Figure 1C and
15 Supp. Figure S1A-C). Under HD, plants phenotypically resembled more heat-stressed plants, e.g.
16 with respect to top area and compactness, however, with a clearly more negative effect (Supp.
17 Figure S1B, S1D). While heat stress caused hyponastic movement of leaves, waterlogging led to
18 an epinastic leaf movement which was accompanied by growth arrest and significant decrease in
19 the top area, compactness and relative growth rate (RGR) that were observed after one day
20 (Figure 1C, Supp. Figure S1A, S1B, S1D, S1E, Supp. Table S3). In the 3rd week, when the single
21 and HD stress treatments were finished (at treatment day 15), plants recovered well from D, H
22 and HD, as reflected by resumption of growth. This trend was not observed for plants subjected
23 to W stress (Figure 1C).

24 Plant performance was the worst in the triple-stress condition (HDW), where 7 days of H were
25 followed by 7 days of combined HD and 7 days of W. Interestingly, during the first three days of
26 W that followed the period of heat and drought plants grew very fast, but with a prolonged stress
27 exposure, plants collapsed, as indicated by RGB side and top view images, the plant volume and
28 growth dynamics as shown in RGR and other measured morphological traits (Figure 1C, Supp.
29 Figure S1, Supp. Table S3).

30 Effect of single and combined stresses on potato physiology

31

1 To evaluate photosynthetic performance under single and multiple stresses, a broad range of
2 physiological traits were extracted from chlorophyll fluorescence images and analysed (Figure 2).
3 Top view images of the operating efficiency of photosystem II (PSII) in light steady state (QY_Lss)
4 clearly showed the negative impact of stress on photosynthetic capacity in all stress treatments,
5 indicated by the reduction of QY_Lss, with D stress causing only a weak negative effect (Figure
6 2A, 2B). Moreover, steady-state fluorescence of maximum efficiency of PSII in the light
7 (F_v/F_m_Lss) showed (only) a significant decrease after 3 days in W alone and when W followed a
8 period of HD till the end of the experiment, indicating a high stress level (Figure 2C, Supp. Table
9 S3). A decrease in steady-state estimation of the fraction of open reaction centres in PSII in the
10 light (qL_Lss) was observed after one day of H and remained consistently lower than in other
11 conditions. In contrast, D had no significant effect on these parameters (Figure 2D, Supp. Table
12 S3). When drought was combined with heat stress (HD), an increase in qL_Lss as compared to
13 H alone was observed. Following H and HD stress, qL_Lss values did not recover back to the
14 control levels at day 21 (Figure 2D), suggesting that photosynthesis is enduringly affected. There
15 was a slow decrease in qL_Lss after long-term W with a clear decline after stress recovery (Figure
16 2D). In addition, changes in canopy temperature (ΔT) were deduced from the thermal imaging,
17 while water use efficiency (WUE) was calculated based on plant volume and water consumption.
18 The rapid increase in ΔT and WUE under W and HDW was most likely caused by rapid stomatal
19 closure (Figure 2E, 2F). The strong response remained over the entire stress period and plants
20 were unable to recover from both stress treatments. A steady increase in ΔT and WUE was
21 observed starting at three days in D, suggesting that the stress was recognised, and the plants
22 responded by closing stomata. When D stress was removed on day 15, the plants recovered
23 immediately (Figure 2E, 2F). Heat stressed plants showed a decrease in ΔT together with an
24 increase in water consumption and a lower WUE, thus indicating enhanced leaf cooling (Figure
25 2E, 2F, Supp. Table S3, S4). During combined HD stress, an intermediate response was
26 observed for these physiological traits compared to single D and H stress.

27 **Stress combinations and waterlogging have strong effects on potato yield**

28 At the end of the phenotyping, plants were harvested to assess the total biomass accumulation
29 and tuber yield (Figure 2G and 2H). Single H stress led to a slightly higher tuber number (Figure
30 2G). However, compared to control conditions, tubers were smaller and weighed less resulting in
31 a lower harvest index. HD also significantly reduced the harvest index compared to control
32 conditions, while D alone did not affect final tuber yield (Figure 2H). W stress strongly inhibited
33 tuber formation and growth and only a few tubers were formed, leading to a significant reduction

1 in the harvest index compared to the control treatment (Figure 2H). A combination of all stress
2 factors abolished tuber formation, reflecting the (near) lethal effect of HDW (Figure 2G, 2H).

3 Negative effects of the stress treatments on tubers were also observed at the metabolic level
4 (Supp. Figure S2). Thus, starch content was significantly lower under H, HD and W stress, while
5 D stress alone has no negative impact. The accumulation of hexoses under H and HD may hint
6 to an increased starch degradation and / or to a reduced starch biosynthesis. W caused a strong
7 accumulation of almost all amino acids, most likely caused by protein degradation and a
8 hampered metabolism (Supp. Figure S2).

9 Molecular responses across omics levels reveal mechanistic insights into 10 multi-stress acclimation

11
12 In addition to the morphological and physiological measurements (68 variables, Figure 3D, Supp.
13 Table S1, S2), leaf samples were taken for parallel multi-omics analysis. The second and third
14 mature leaf per plant were pooled, homogenized and used for further analysis (Figure 3A). For
15 each of the treatments the fast response (one day post treatment) and the status at the end of a
16 prolonged stress duration (7 or 14 days of stress) was investigated (sampling points see Figure
17 1A). While the proteome analysis was untargeted (4258 identified proteins, Supp. Table S5, S6),
18 other omics analyses were targeted comprising 14 pre-selected transcriptional marker genes
19 involved in stress response and tuberization, 13 phytohormones encompassing abscisic acid,
20 ABA; jasmonic acid, JA; salicylic acid, SA; indole-3-acetic acid IAA, and their derivatives as well
21 as 22 metabolites encompassing amino acids and sugars (Supp. Table S4). To identify processes
22 regulated on proteomics level we performed gene set enrichment analysis (GSEA, Supp. Table
23 S6).

24 A multi-level data integration protocol was developed to investigate plant signalling/responses
25 across the different omics levels (Figure 3B). First, we investigated data distribution by
26 multidimensional scaling (Figure 3C, Supp. File S1). This graph shows a clear clustering aside of
27 samples taken after 7 and 8 days of waterlogging. Therefore, only data from the first week of
28 waterlogging were included in further analyses, taking also into consideration that after two weeks
29 of waterlogging all plants were severely damaged. The overview of data distribution also revealed
30 that the most distant physiological state was that of plants exposed to triple stress (HDW): first
31 one week of heat, followed by one week of heat combined with drought, and finally one week of
32 waterlogging (Figure 3C). Because the triple stress treatment turned out to be very harsh and

1 plants were severely affected in both above ground and below ground growth, we also excluded
2 data from these samples from all further analyses. Next, we reduced the number of variables
3 obtained on phenomics and proteomics levels to equalise numbers of variables across different
4 analysed levels. In order to identify the most informative variables, feature selection using random
5 forest with recursive feature elimination was conducted on the phenomics data, keeping 6
6 variables for downstream analysis (Figure 3D: qL_{Lss} , F_v/F_m_{Lss} , top area, ΔT , compactness
7 and water consumption). The proteomics dataset was reduced to keep only proteins that were
8 identified as differentially abundant in any comparison of stress vs. control (135 proteins) and
9 were functionally assigned to pathways that were studied also on other levels (36 proteins, related
10 to photosynthesis, metabolism of sugars and amino acids, hormone metabolism and signalling,
11 ROS signalling and stress pathways).

12 In addition, correlation analysis within each level of omics data was performed, revealing that
13 these components are only weakly connected in control conditions, while in both heat or drought,
14 they are highly correlated to each other (see e.g. for hormones and transcripts, Supp. Figure S3A,
15 S3B). More severe stresses, such as the combined heat and drought stress and waterlogging,
16 however, broke this link, suggesting a disorganisation of signalling responses. The canonical
17 correlation analysis between components of different molecular levels similarly showed low
18 connection in control samples. In stressed samples, blocks of components appeared to be
19 strongly regulated, each specific to a particular stress (Supp. Figure S3C).

20 Variables measured on different omics levels were integrated into a metabolism and signaling
21 cascade-based knowledge network to capture events at the molecular level (Figure 4A). Finally,
22 we superimposed the measured data onto this mechanistic knowledge network and visualised
23 them in parallel for all omics levels per each analysed condition compared to control (Figure 4B,
24 Supp. Table S3, Supp. File S2). This provides a comprehensive overview of how these stresses
25 rewire biochemical pathways and physiological processes. These networks were used for
26 interpretation of processes in single and combined H and D stress as well as for W, and are
27 described in the subsequent sections.

28 **Metabolic and molecular responses to individual and combined heat- and** 29 **drought stress exhibit combinatorial and distinct signatures**

30 While heat stress was effective immediately, drought stress, applied by water withdrawal on day
31 seven in our setup, became effective gradually within three days, visible by an increase in the ΔT
32 values (Figure 2E). Like previous reports (Demirel et al., 2020; Zaki and Radwan, 2022), we found

1 that Désirée was moderately drought tolerant and exhibited only minor morphological and
2 physiological responses at the moderate stress level applied in our study (30% field capacity) and
3 the plants fully recovered when the stress treatment was finished. The potato plants clearly
4 responded to elevated temperatures (H) with morphological adaptation like the upward movement
5 of leaves (Figure 1C), which is part of thermomorphogenic responses (Quint et al., 2016).
6 Previous work showed that heat stress caused an altered biomass allocation between shoots and
7 tubers of potato plants, with less assimilates allocated to developing tubers (Hancock et al., 2014;
8 Hastilestari et al., 2018). Decreased tuber yield (higher number of tubers with smaller biomass,
9 Figure 2G) and starch accumulation, leading to a lower harvest index, were also observed in our
10 study (Figure 2H and Supp. Figure S2).

11 To investigate the effect of heat and/or drought stress on leaf carbohydrate metabolism, contents
12 of soluble sugars and starch were measured (Figure 5A). While sucrose levels did not change
13 (Supp. Table S3), there was an about twofold increase in the amount of fructose and glucose
14 after 14 days of H and at day 7 of D and HD. Under H and HD combination also less starch
15 accumulated in leaves (Figure 5A). This most likely reflects the decreased photosynthetic
16 assimilate production and contributes to a lower amount of carbon that can be transported to sink
17 organs, such as growing tubers to stimulate growth and starch deposition. The soluble sugars
18 may act as osmoprotectants under these stress conditions, feed the increased demand for energy
19 and serve as building blocks for stress defence responses. Accordingly, we found that, enzymes
20 involved in glycolysis or sucrose degradation were upregulated in H and combined HD stress as
21 indicated by gene set enrichment analysis which summarizes the complex proteomics data set
22 (Figure 5D and Supp. Table S6).

23 Expression of the sugar efflux transporter *SWEET11* was upregulated at the end of both H and D
24 stress presumably to maintain sucrose loading into the phloem and carbon allocation to sink
25 tissue to counterbalance the decreased carbon assimilation rate of source leaves. This view is
26 supported by various other studies demonstrating an emerging role of SWEET sugar transporters
27 in abiotic stress responses as summarized in (Gautam et al., 2022). For example, Chen and co-
28 workers showed that *AtSWEET11/12* are rapidly activated under drought stress in an ABA and
29 SNF1-related protein kinase 2.9 (Snrk2)-dependent manner to enhance assimilate allocation from
30 shoot to root to stimulate root growth and allow stress adaptation (Chen et al., 2022). One key
31 player stimulating tuberization and tuber growth is the tuberigen *SP6A*. Its expression was
32 downregulated during the first week of H and in combined HD (Figure 5C). During longer heat
33 exposure, expression levels of *SP6A* were similar to control levels, but remained low in HD.
34 Drought alone had little effect on *SP6A*, which is consistent with the low impact on final tuber yield.

1 In potato, the transcriptional regulator protein *Constans-like 1* (CO) was described to act as a
2 negative regulator of *SP6A* expression (Abelenda et al., 2016). CO was upregulated within 7 days
3 of drought stress (D), and it increased with longer durations of heat, but was unaffected by HD
4 combination (Figure 5C). Hence, in our experiment, the transcript levels of CO did not always
5 change in the opposite direction as *SP6A*, suggesting additional regulatory mechanisms may act
6 under stress conditions.

7 Considering the changes in amino acids, the most striking finding was the strongly elevated levels
8 of histidine (His) in all three stress treatments, with the highest amounts detected in combined HD
9 stress (Figure 5A). This was accompanied by a significant increase of many (minor) amino acids,
10 in particular isoleucine (Ile) and other branched chain amino acids (BCAs). This observation was
11 in line with previous reports on combined heat- and drought stress in potato (Demirel et al., 2020),
12 although its cause and physiological importance need further investigations. Accordingly, at the
13 proteome level, proteins involved in BCA synthesis were significantly enriched among the ones
14 with increased levels in stress (Figure 5D, 5E, Supp. Table S5, S6).

15
16 Proline is an established regulator of osmotic potential that protects cells by stabilizing proteins
17 and scavenging ROS. Proline levels increased at day 7 of D stress (sampling day 14) (Figure 5A).
18 This was consistent with increased transcript levels of the *delta-1-pyrroline-5-carboxylate*
19 *synthase 1* (*P5CS*), the key enzyme for proline synthesis, and of *Responsive to Desiccation 29B*
20 (*RD29B*), both being well-known stress marker genes. In line with these findings, the levels of
21 ABA, the key phytohormone that induces stomal closing, proline accumulation and other drought
22 stress responses (Cutler et al., 2010; Zhang et al., 2022), were elevated after 7 days of D but
23 were clearly reduced in H, while no changes were detected in HD stress. Interestingly, the levels
24 of phaseic acid (PA), and dihydrophaseic acid (DPA), two breakdown products of ABA, were lower
25 at one day of D but significantly higher after 7 days in D. The strongest accumulation of DPA
26 levels was detected in the HD treatment, in which DPA levels were elevated already after one day
27 and further increased until the end of the treatment (at day 7). The elevated levels after one day
28 of HD can be explained by the experimental setup, in which the D treatment started after 7 days
29 of H (that also resulted in DPA accumulation). However, the strong accumulation of ABA
30 breakdown products under D and to even higher levels in HD are in line with their suggested role
31 in long-term stress acclimation. PA, the first degradation product of ABA and precursor of DPA,
32 is known to activate a subset of ABA receptors (Weng et al., 2016). Because ABA has a very
33 short half-life, it was suggested that the long-lived PA could prime plants for enhanced responses
34 to future drought (Lozano-Juste and Cutler, 2016).

1
2 The phytohormone JA is another typical stress hormone known to be involved in many biotic but
3 also abiotic stress responses (Wasternack and Feussner, 2018). We found strongly increased
4 levels of the biologically active form jasmonyl-L-isoleucine (JA-Ile) under H, D and HD conditions
5 (Figure 5B). 12-Hydroxyjasmonic acid (12-OH-JA) is a by-product of switching off JA signaling
6 with weak signaling activity (Nakamura et al., 2011). It was also described to function as tuber-
7 inducing factor in potato (Yoshihara et al., 1989). Under H, amounts of 12-OH-JA and free JA
8 switched from higher amounts measured at day 1 to lower levels at day 8, and decreased further
9 till the end of the experiment. Also, *cis*-12-oxo-phytodienoic acid (*cis*-OPDA), the biochemical
10 precursor of JA, was detected at much lower levels on day 8 and 14 in H. *Cis*-OPDA was also
11 reduced at the start of the combined HD (day 1) treatment, most likely because of prior heat
12 treatment. Altogether, this indicates a strong upregulation in the last step of conjugation for the
13 synthesis of JA-Ile in H, D and HD.

14
15 The accumulation of ROS is a detrimental by-product of photosynthesis and other metabolic
16 pathways under stress conditions. Accordingly, ROS detoxification by different enzymes such as
17 catalases or superoxide dismutases, together with induction of Ca²⁺ signals, is a typical response
18 emerging from stressed chloroplasts (Stael et al., 2015). In line with that, we measured increased
19 transcript levels of *CATALASE 1 (CAT1)* and a methyl esterase (*MES*), which was selected as
20 Ca²⁺ signaling marker gene (M. Knight, unpublished data), at the end of the drought and heat
21 treatment (sampling day 14). The transcript levels of *pathogenesis-related protein 1b1 (PR1b)*, a
22 biotic stress as well as drought and salt stress marker (Akbulak et al., 2020) were first lower in H
23 but increased from day 8 to 14 in H and at day 7 in D (Figure 5C). A similar response was seen
24 for the chloroplast-localized *13-lipoxygenase (St 13-LOX3.1)*, which is a well-known marker gene
25 for different stresses, especially chloroplast generated ROS (Bachmann et al., 2002) suggesting
26 increased ROS formation and stress level with stress duration. Strikingly, the expression of these
27 genes was less induced or even inhibited when H and D were combined, which may indicate the
28 activation of opposing signaling pathways.

29
30 Heat stress, but also other stresses, induces the production of heat-shock proteins (HSPs), which
31 is a very conserved process in all organisms. HSPs act as molecular chaperones and play an
32 important role in maintaining cellular homeostasis and the proteome by supporting protein folding,
33 preventing misfolding or by assisting in the degradation of irreversibly damaged polypeptides
34 (Sato et al., 2024). At the transcript level, we observed clearly elevated levels of the *heat shock*

1 *protein 70 (HSP70)* after single H and D stress. Under H this was accompanied by an
2 accumulation of numerous HSP proteins as indicated by their significant enrichment among the
3 identified proteins in the proteome approach (Figure 5D, 5E). This effect was similarly pronounced
4 in combined HD stress (Figure 5E) with a strong enrichment of HSP70, HSP90, and HSP101
5 involved in heat stress responses and protein folding (Figure 5D). The category “protein folding”
6 comprises mainly HSP70 and 60 group members many of which are present in the chloroplast,
7 where they participate in the repair of PSII components, but also protect enzymes such as
8 Ribulose-1,5-bisphosphate carboxylase/oxygenase (RuBisCo). In fact, our physiological data
9 indicate a disturbance in the electron-transport chain through PSII under heat. For example, we
10 saw a strong decrease of PSII efficiency under H stress (Figure 2B). The negative effect of H
11 stress is also reflected in lower abundance of PSII proteins in the gene enrichment analysis
12 (Figure 5D). More specifically (Supp. Table S5), there were reduced amounts of the PsbQ and
13 PsbP subunits of the oxygen-evolving complex.

14
15 Overall, we do see specific stress responses to heat and drought, but also to a combination of
16 both. This is evident in Figure 5E illustrating the signature of responses elicited by combined heat
17 and drought stress in biochemical pathway view (knowledge network overlaid with multi-omics
18 data). The responses to HD only partly overlap with single D stress, e.g. for the accumulation of
19 DPA. However, for most of the measured metabolites, the patterns were similar to those observed
20 under heat stress, with changes being more pronounced under HD (Figure 5E). Here, we cannot
21 exclude that this domination by heat was linked to the rather mild drought stress. Interestingly,
22 the transcriptional changes of selected stress-related enzymes were weakest in HD stress
23 combination pointing to a redirection and rearrangement of signaling pathways compared to
24 individual stress factors as suggested by other studies (Zhang and Sonnewald, 2017).

25 Comprehensive insight into molecular processes mediating the extreme 26 waterlogging sensitivity of potato

27 Despite being documented as a highly flood-sensitive species, an in-depth characterization of
28 flooding-induced stress responses in potato is sparse (Jovović et al., 2021). The waterlogging
29 sensitivity of potato was evident in the HTP data, with several morpho-physiological traits related
30 to plant performance being negatively impacted following stress imposition (Figure 1C, Figure 2).
31 This included: leaf epinasty, decreased biomass accumulation and shoot elongation, impaired

1 photosynthesis and stomatal conductance as well as a dramatic reduction of tuber yield (see
2 Figure 1,2).

3 Waterlogging significantly affected primary metabolic pathways as reflected in an increase in
4 soluble sugars and free amino acids (Figure 6A). We also observed changes in the expression of
5 stress-associated genes and hormones, thus highlighting potential mechanisms involved in
6 waterlogging acclimation. These include the increase of ABA (ABA, PA, DPA) metabolism and
7 response (*RD29B*), as well as the upregulation of the ethylene (ET) biosynthesis gene, 1-
8 aminocyclopropane-1-carboxylate oxidase 2 (*ACO2*), and the ROS-producing enzyme,
9 respiratory burst oxidase homolog A (*RBOHA*). Waterlogging also resulted in the accumulation
10 of various JA metabolites, 9,10-dihydrojasmonic acid (9,10-dHJA), cisOPDA, and JA-Ile, along
11 with the upregulation of *13-LOX3.1*, an enzyme involved in JA metabolism. The strong ABA
12 signature observed in waterlogged plants prompted us to compare waterlogging and drought
13 responses (Figure 6B). This revealed common stress-associated responses (e.g.: the induction
14 of *ACO2*, *RD29B*, *HSP70*) and a much stronger ABA response in waterlogging relative to drought.
15 Another notable observation was the upregulation of the tuberigen signal, *SP6A* after 1 day of
16 waterlogging, coinciding with the downregulation of its negative regulator *CO* (Figure 6C).

17 Proteomics analyses of waterlogged plants revealed mild effects. Six differentially enriched
18 proteins were identified in response to prolonged (7 days waterlogging, W07) waterlogging
19 treatment. Among the strongly upregulated proteins, were a leucyl aminopeptidase 2-like (LAP2-
20 like) (VdnPW4_5460), two glucan endo-1,3-beta-glucosidases (VdnPW4_8729, PBdnRY1_427),
21 a Pollen-Pistil Incompatibility 2-like protein (POP2-like) encoding a gamma-aminobutyric acid
22 (GABA) transaminase and a component of the coat protein complex II, SECRETORY31B-like
23 protein (SEC31B-like), involved in vesicular transport from the endoplasmic reticulum (ER) to the
24 Golgi apparatus (Li et al., 2021). Waterlogging led to the downregulation of the chloroplast
25 RIBOSOMAL PROTEIN L27A-like (RPL27-like), demonstrated to be important for protein
26 synthesis (Figure 6D).

27 The multi-level integrative analyses enabled visualization of the progression of stress symptoms
28 in waterlogged plants. In comparison to one day of waterlogging, molecular responses to
29 prolonged waterlogging stress displayed a distinct signature (Figure 6E). While ABA-, JA- and
30 ROS-biosynthesis and accumulation of free amino acids was further increased, we observed that
31 prolonged waterlogging led to a general inhibition of the tuberization process (i.e. *SP6A*
32 downregulation). In addition, genes related to ethylene biosynthesis (*ACO2*) and response
33 (ETHYLENE RESPONSE FACTOR1, *ERF1*) were no longer found to be transcriptionally

1 upregulated, thus suggesting temporal control of ethylene signaling. Despite representing
2 opposite ends of the water stress spectrum, waterlogging and drought, elicited significantly
3 overlapping responses, notably related to ABA metabolism and proline accumulation (Figure 6A,
4 6B, 6E).

5 DISCUSSION

6 Despite its outstanding importance as a major food crop, research into the vulnerability of potato
7 to abiotic stresses lags that of other staple crops. In recent years, potato yields have been
8 significantly affected by heat, drought, and flooding, often occurring sequentially or simultaneously
9 (Dahal et al., 2019; Jovović et al., 2021; von Gehren et al., 2023). Considering the increasing
10 occurrence of these extreme weather events, this knowledge gap needs to be urgently addressed.
11 In this study, we leveraged the power of several omics techniques and their integrated analysis
12 to build a comprehensive global picture of potato responses to single and combined heat, drought,
13 and waterlogging stress.

14

15 **Leveraging multi-omics data integration to capture the complexity of biological systems**

16

17 Several tools have already been developed for integrative analysis of multi-omics data (Joshi et
18 al., 2024). Most broadly used are the mixOmics package (Rohart et al., 2017; Singh et al., 2019),
19 integrating datasets based on correlations, and the pathway visualisation tool PaintOmics (Liu et
20 al., 2022). In this study, however, we integrated five omics-level datasets. Such complex datasets
21 have rarely been analysed, even in medical research (Lee et al., 2019), as most studies combine
22 only two to three omics datasets (Ployet et al., 2019; Lozano-Elena et al., 2022; Núñez-Lillo et al.,
23 2023; Núñez-Lillo et al., 2024; Sinha et al., 2024). Since existing tools were not directly suitable
24 for our needs, we developed a pipeline harnessing the potential of both integrative and
25 visualization approaches. An additional step, based on machine learning, was introduced to
26 reduce the number of variables, in particular of phenotypic physiological data. This reduction of
27 variables was especially important for the correlation analyses across omics levels, where we
28 kept only the most informative variable. In the first step we performed statistical modelling and
29 correlation analyses, which provided partial overview of events. In the second step, mechanistic
30 insights were obtained by generating a customised biochemical knowledge network. Our network
31 was constructed based on knowledge extracted from different databases, most notably the Stress
32 Knowledge Map (Bleker et al., 2024) and KEGG (Kanehisa et al., 2017), as well as from literature,

1 to integrate all components that were kept after variable selection. The obtained biochemical
2 knowledge network enabled a comprehensive overview of events at the pathway level and led to
3 the identification of mechanistic differences occurring in response to different stresses. The
4 developed pipeline is thus highly useful for integration and interpretation of complex datasets in
5 future studies and can also be applied to other species.

7 **Integrative omics provides global insights into potato abiotic stress responses**

8
9 Multi-omics approaches have been successfully applied in numerous crop species to better
10 understand abiotic stress responses. Our study does so in potato by subjecting the cultivar
11 Désirée to waterlogging, drought, heat, a combination of heat and drought, and triple stress
12 combination encompassing all three. Across each stress treatment, detailed morpho-
13 physiological traits were measured, with a subset of plants sampled for the probing of a diverse
14 array of molecular stress markers, hormones, metabolites, and proteome analyses across several
15 time points.

16
17 In general, stress combinations appeared to be more detrimental to the plant performance than
18 individual stress applications. The combination of H, D and W led to a rapid decline in plant
19 viability and eventually most plants died. However, all individual stress factors caused a reduced
20 plant growth, had a negative impact on photosynthetic assimilate production, and both heat and
21 waterlogging stress impaired tuber yield (Figure 7) and tuber starch accumulation (Supp. Figure
22 S2). Considering all stress responses, it turned out that the cultivar Désirée was less affected by
23 the applied drought stress indicating that it is quite resilient to drought as suggested previously
24 (Demirel et al., 2020). A combination of heat and drought caused stronger growth retardation than
25 both stresses alone with drought responses overwriting heat adaptations.

26 Nevertheless, despite the apparent mild drought phenotypes, a clear drought-associated
27 signature (accumulation of ABA, sugars, proline, histidine and most stress-induced transcripts)
28 confirmed the activation of stress responsive pathways, particularly at day 7, which contributed to
29 stress acclimation (Figure 5). Thus, there was a clear activation of the ABA response pathway,
30 as seen by an increase in the content of the hormone and its degradation products, as well as
31 proline, and the increased expression of ABA-responsive marker genes *SnRK2*, *P5CS*, *RD29B*,
32 leading to the corresponding physiological responses, e.g. a decreased water-use and leaf
33 temperature caused by stomata closure. Particularly interesting was the accumulation of the ABA
34 catabolite DPA after longer drought stress. The precursor of DPA, PA was suggested to have an

1 important role in priming for increased resilience to future drought stress in *Arabidopsis* (Lozano-
2 Juste and Cutler, 2016). It is believed that DPA does not trigger ABA responses, but that has to
3 our knowledge not been studied in potato. Hence, it might be that DPA acts as priming signal for
4 stress acclimation and resilience in potato.

5
6 Compared to drought, heat stress had a stronger impact on Désirée plants at all levels from
7 growth to photosynthesis and yield. Thermomorphogenesis is a well-described morphological
8 response to elevated temperature stress comprising shoot elongation and hyponastic movement
9 of leaves which together with an increased transpiration are seen as an acclimation to increase
10 ventilation and to cool the aboveground part (Quint et al. 2016). In our study we clearly observed
11 the hyponastic movement of leaves and stomatal opening, indicated by a decrease in ΔT (Figure
12 7). This physiological response was accompanied by a decreased amount of ABA. In contrast,
13 the heat-mediated shoot elongation that has been seen in other potato varieties was not visible
14 in Désirée (Hastilestari et al., 2018; Tang et al., 2018). Instead, the plant height of Désirée plants
15 was reduced under elevated temperature suggesting cultivar-specific difference that could be
16 exploited in further studies to untangle different morphological stress adaptation mechanisms in
17 potato. In *A. thaliana*, the thermomorphogenetic hypocotyl elongation is tightly linked with an
18 increase in auxin levels and is mediated by the transcription factor Phytochrome interacting factor
19 4 (PIF4) (Quint et al. 2016). Consistent with the morphological response, we did not find
20 significantly altered levels of the phytohormone IAA in leaves of Désirée plants in response to
21 heat (Figure 5B).

22
23 High temperature treatment negatively affects photosynthetic capacity, particularly the efficiency
24 of photosystem II, which is in line with results of other studies (Mathur et al., 2014), and this was
25 confirmed here at both physiological and proteomic level. In a previous study by (Hancock et al.,
26 2014), which also used cv. Désirée, the net CO₂ assimilation was even higher under elevated
27 temperatures than in control conditions. This difference might be related to the different setup, as
28 in the latter study the night temperature was kept at 20°C, while here it was adjusted to 28°C,
29 suggesting that a low night temperature is important to maintain photosynthetic activity. The heat-
30 induced impact on photosynthetic capacity most likely caused a lower production of assimilates,
31 indicated by the decreased amount of transitory starch in leaves. Concomitantly, contents of
32 hexoses were found to be increased consistent with earlier studies (Hastilestari et al. 2018). This
33 increase may contribute to the osmoprotection of cells and provides energy for the costly heat
34 stress response such as the formation of heat shock proteins (Guihur et al., 2022). A massive

1 accumulation of heat shock proteins was found after one week of heat stress, together with
2 elevated levels of *HSP70* transcript levels at day 8 (Figure 5C). Although energy-demanding, the
3 transcriptional induction of *HSP* is important for the cellular homeostasis and maintenance of
4 growth and metabolism at elevated temperature. This is well demonstrated by transgenic potato
5 plants with increased expression of a beneficial allele of *HSP70*, that exhibit improved heat stress
6 tolerance (Trapero-Mozos et al., 2018).

7
8 A downregulation of photosynthesis is a typical stress response to prevent potential damage, for
9 example caused by ROS. This has strong implications on plant growth and yield and is therefore
10 regulated at various levels including light-harvesting and electron transport with high implications
11 for crop improvement (Kromdijk et al., 2016), particularly under stress conditions (Grieco et al.,
12 2020). The resulting lower photosynthetic capacity together with an increased energy demand for
13 stress defense reduces the amounts of assimilates that can be translocated toward the
14 developing tubers and its availability for storing starch. In addition to assimilates, molecular
15 signals play a critical role in stimulating tuber development and growth. One important regulator
16 is *SP6A* which was downregulated at the transcript level in our study, consistent with previous
17 findings (Hancock et al., 2014; Lehretz et al., 2020; Park et al., 2022; Koch et al., 2024). The
18 downregulation of *SP6A* likely contributes to the observed reduction in tuber yield under stress
19 conditions. Notably, stem-specific overexpression has been shown to overcome heat-mediated
20 yield reduction by enhancing delivery of assimilates to developing tubers, thereby improving tuber
21 growth and starch accumulation.

22
23 Looking at plant hormones, we observed changes of stress hormones like SA and JA, that
24 traditionally have been associated with biotic stress responses. Quite striking in this context was
25 the increase in the amount of JA-Ile under heat, drought and the combination of both (Figure 5B).
26 This is consistent with previous observations reporting that JA has a positive effect on
27 thermotolerance in *Arabidopsis* (Clarke et al., 2009; Balfagon et al., 2019). Heat stress increased
28 levels of OPDA, JA and JA-Ile and application of 5 μ M methyl-jasmonate improved cell viability
29 (Clarke et al., 2009). Using various mutants, this study also showed that JA acts in concert with
30 SA in conferring thermotolerance. Moreover, an accumulation of JA-Ile was also observed in
31 *Arabidopsis* under drought (Yoshida and Fernie, 2024), and increased levels of JA-Ile by
32 overexpression of *JASMONATE RESISTANT1 (JAR1)* resulted in improved drought stress
33 tolerance, but in stunted growth (Mahmud et al., 2022). Detailed analyses of how levels of JA and
34 its derivatives as well as biosynthesis and signaling components change in response to stress

1 are still missing in potato. Therefore, a deeper understanding of regulatory factors is required,
2 particularly the crosstalk with other hormones and the impact on plant growth. However, a tight
3 modulation of JA metabolism seems like a promising target for future engineering of abiotic stress
4 tolerance in potato (Bittner et al., 2022).

5 6 **Extreme sensitivity to waterlogging in potato – integrative -omics highlights** 7 **commonalities with drought**

8
9 Our study provides detailed insight into the molecular responses underlying the high vulnerability
10 of potato to waterlogging. Water saturation imposes rapid oxygen deficiency in the soil, thus
11 impairing root respiration and function. Plant survival in flooded soils involves various
12 morphological and metabolic responses to either escape or cope with hypoxia, which involve
13 acclimation responses in roots but also in aerial organs (Sauter, 2013; Leeggangers et al., 2023).
14 The data showed that plant growth and performance were more drastically affected by
15 waterlogging as compared to H, D and HD treatments. In addition, HTP data suggests that
16 waterlogging had a dominant effect even when applied after a previous combined exposure to
17 heat and drought (HDW) (Figure 1C and 2). When applied as a single stress, detrimental effects
18 on plant performance increased over time. Waterlogging dramatically impairs root conductance
19 and water and nutrient uptake, causing tissue dehydration and wilting. This triggers water-saving
20 responses such as stomatal closure and epinasty, which were reflected in increased leaf
21 temperatures and reduced plant compactness, respectively (Figure 1, 2E, suppl. Figure 1).
22 Epinastic leaf movement, a common waterlogging response in Solanaceae, is thought to reduce
23 photosystem damage by irradiation and transpiration (Jackson and Campbell, 1976; Geldhof et
24 al., 2023). Both stomatal conductance and epinasty are regulated by the pivotal flooding signal
25 ethylene (Leeggangers et al., 2023). While ethylene levels were not measured here, the analyses
26 of synthesis genes (i.e.: *ACO2*) suggested the activation of ethylene production in waterlogged
27 shoots. Ethylene is also known to trigger *RBOH* expression and can act synergistically with ABA
28 to reduce stomatal conductance (Zhao et al., 2021). ABA is also considered to signal root stress
29 during waterlogging (Jackson and Hall, 1987; Zhao et al., 2021). We observed both the activation
30 of ABA signaling and ABA accumulation, which together with increased levels of proline, indicates
31 a strong drought signature (Figure 6A, 6B, 6E). While paradoxical, waterlogging is known to elicit
32 shoot drought responses. As root function in hypoxic soil ceases, it triggers a ‘drought-like’
33 response in the shoot with the similar goal to trigger water saving measures. A focus on this ABA

1 and drought-mediated regulatory network might thus be an attractive target for probing common
2 resilience mechanisms to both drought and waterlogging.

3 The energy shortage caused by waterlogging also leads to significant changes in sugar
4 metabolism. The accumulation of soluble sugars such as glucose and fructose, might be a
5 consequence of sink-source imbalances during waterlogging and thereby, a decline in shoot-to-
6 root sugar transport. Strikingly, after one day of waterlogging, we observed upregulation of *SP6A*,
7 a positive regulator of tuberization, thus suggesting potential roles of this gene in short-term
8 responses to waterlogging.

9
10 Prolonged exposure to waterlogging revealed several aspects of late responses and factors
11 contributing to potato susceptibility to waterlogging. Leaves of waterlogged plants overcome
12 energy shortages by recycling carbon from amino acids and GABA. The latter plays an important
13 role not only in TCA replenishment but also in ion homeostasis and reduction of oxidative stress
14 (Lothier et al., 2020; Wu et al., 2021). We observed a strong increase in free amino acids that,
15 together with the upregulation of POP2 and an aminopeptidase (Figure 6), suggests increased
16 protein breakdown and utilization of amino acids as alternative energy sources. Furthermore, the
17 downregulation of RPL27 (and other ribosomal proteins) could indicate the shutting down of
18 energy-demanding processes, such as protein synthesis, as a response to this energy shortage.

19
20 Potato susceptibility to prolonged waterlogging was evidenced by other multi-level events such
21 as the upregulation of proteins related to protein and cell wall component turnover, *RBOHA*
22 upregulation and photosynthesis impairment (Figure 2, Supp. Figure S3, Figure 6). It is also
23 explained by increased ABA signaling and biosynthesis and *RBOHA* expression, which
24 convergently indicate increased tissue dehydration and oxidative stress that is reflected in the
25 HTP data (Figure 1C, Figure 2). This includes decreased tuber number and weight, indicating a
26 retardation of both tuber initiation and bulking. As tuberization is a particularly energetically
27 expensive process, the imposition of root zone hypoxia likely disrupts the underground sink force
28 essential for stolon development, tuber initiation and bulking.

29
30 Altogether, our data suggest that two weeks of waterlogging led to near-lethal effects, and even
31 if acclimation responses were activated, overall, they could not compensate for maintaining root
32 function (i.e. unrecovered water consumption, Supp. Table S4) and general plant survival, even
33 during recovery, thus confirming the high susceptibility of potato to waterlogging.

34

1 **Conclusions**

2 The present comprehensive approach produced a rich integrated dataset, which enabled diverse
3 exploration of molecular mechanisms across various levels and processes. Through the
4 connection of phenotype to molecular responses, we attained deeper insights into the intricate
5 regulation of metabolic and phenotypic traits. This should now guide the identification of key
6 regulators that govern the interplay between molecular dynamics and their phenotypic
7 expressions. The utilization of both knowledge-based approaches and multivariate statistical
8 methods played a crucial role in deciphering complex molecular regulatory networks and their
9 association with phenotypic and physiological traits, thereby facilitating the rapid generation of
10 hypotheses.

11 In addition to several insights into potato stress responses, this study also provides a blueprint for
12 performing and analysing single and multiple stress and effective integration of large datasets for
13 potato. Importantly, this setup can also be applied to other plant species. These advancements
14 hold significant implications for potato breeding strategies, providing a deeper understanding of
15 plant stress responses and expediting trait selection. As agricultural landscapes confront
16 challenges like climate change and population growth, embracing multi-omics integration holds
17 promise for cultivating resilient potato varieties that can thrive in various conditions.

18 **MATERIALS AND METHODS**

19 **Plant growth conditions and sampling**

20 150 in-vitro potato cuttings (*Solanum tuberosum* cv. Désirée) were cultivated and grown as
21 described in the supplementary methods. After 32 days of cultivation, plants were randomly
22 distributed into 6 groups (6 plants each) referring to control group and 5 different stress conditions
23 (heat, drought, combined heat and drought, waterlogging and combination of heat, drought and
24 waterlogging) (Figure 1). Plants were moved into two growth units of Growth Capsule (PSI;
25 (Photon Systems Instruments), Czech Republic) where climate conditions for day/night
26 temperature were set in one unit to 22/19°C, referring to control conditions, and in the second unit
27 to 30/28 °C, referring to heat conditions. In both units growing light intensity was set at 330 μmol
28 $\text{m}^{-2} \text{s}^{-1}$ PPFD and relative humidity was maintained at 55%. All plants were measured under
29 control in day 0 then the stress treatments depicted schematically in Figure 1. The treatments
30 were applied as the following: (1) Control conditions – cultivation at 22/19 °C, watering up to 60%
31 FC; (2) Drought conditions – cultivation at 22/19 °C, watering up to 60% FC until day 7, then

1 reduce watering to 30% FC for 1 week (until day 14); (3) Heat conditions – cultivation at 30/28 °C
2 for 2 weeks, watering up to 60% FC until day 14; (4) Heat + Drought conditions - cultivation at
3 30/28 °C for 2 weeks, watering up to 60% FC for 1 week (until day 7), then reduce watering to
4 30% FC for 1 week (until day 14); (5) Waterlogging conditions – cultivation at 22/19 °C, watering
5 up to 130% FC for 2 weeks (until day 14); (6) Heat + Drought + Waterlogging conditions –
6 cultivation at 30/28 °C for 2 weeks with watering up to 60% FC for 1 week (until day 7), then
7 reduce watering to 30% FC until day 14 followed by inducing waterlogging by cultivation at
8 22/19 °C for 1 week with watering up to 130% FC until day 21. Except for Heat + Drought +
9 Waterlogging conditions, all stress treatments were followed by one week of recovery (from day
10 15 and until day 21) in control conditions.

11 Plants were divided into two sets, “phenotyping plants” and “plants for tissue harvest” (see Supp.
12 Table S1). Phenotyping set consisted of 6 replicates per treatment, in total 36 plants, and was
13 used for daily image-based phenotyping (for definition of scored traits see Supp. Table S2).

14 High-throughput phenotyping

15 Prior to the stress treatment initiation and during the stress treatments, all plants were daily
16 phenotyped. A comprehensive phenotyping protocol was used for the acquisition of physiological
17 and morphological traits according to the described method (Abdelhakim et al., 2024). All imaging
18 sensors for digital analysis are being implemented in the PlantScreen™ Modular system (PSI,
19 Czech Republic). The photosynthesis-related traits were determined using kinetic chlorophyll
20 fluorescence imaging where the selected protocol for measuring plants was similar to the defined
21 approach (Abdelhakim et al., 2024). The measurement of temperature profiles of the plants was
22 measured using thermal imaging, where the acquisition and segmentation of the images were
23 processed as described in (Abdelhakim et al., 2021; Findurová et al., 2023). The morphological
24 and growth dynamics were determined using both top and multiple angles (0°, 120°, and 240°)
25 side view RGB imaging, and images were processed as described by (Awlia et al., 2016). Each
26 pot was loaded onto a transport disk automatically moving on a conveyor belt between the
27 automatic laser height measuring unit, acclimation unit, robotic-assisted imaging units, weighing
28 and watering unit, and the cultivation greenhouse located area. The raw images were
29 automatically processed and parameters were extracted through PlantScreen™ Analyzer
30 software (PSI, Czech Republic) (Supp. Table S2). Statistical evaluation was performed to check
31 the differences between the treatments using Wilcoxon test (Supp. Table S3).

1 Tissue sampling

2 Leaf sampling was conducted on days 1, 7, 8, 14, 15, and 21 after stress treatment initiation
3 (Treatment days). The 2nd and 3rd fully developed leaves were harvested and flash-frozen in liquid
4 nitrogen. Subsequently, leaf tissue was homogenised, aliquoted and distributed for individual
5 follow-up proteomics, and targeted transcriptomics, metabolomics, and hormonomics analyses.
6 Remaining above ground tissue was harvested and total fresh weight (FW) and dry weight (DW)
7 was measured (Supp. Table S4). In total 112 plants with 4 replicates per sampling time and per
8 treatment were collected. The 4th leaf was harvested to calculate relative water content (RWC)
9 (Supp. Table S4), and three leaf disks were collected and weighed, then soaked in water to
10 determine the turgor weight (TW) and dried in the oven to calculate RWC (Supp. Table S2). In
11 addition, at the end of the experiment, the below ground tissue was collected, where number of
12 tubers per plant and total weight were assessed from four replicates per treatment. Harvest index
13 was calculated as a ratio between tuber weight and the total biomass.

14 Multi-omics analysis

15 Transcriptomic marker analysis

16 RT-qPCR was performed to assess the expression of 14 marker genes involved in redox
17 homeostasis, hormonal signaling (ethylene, cytokinin, ABA, SA, and JA), heat stress, tuber
18 development, circadian clock, and calcium signaling using previously validated reference genes
19 (Supp. Table S7).

20 RNA was extracted and DNase treated using Direct-zol RNA Miniprep Kit (Zymo Research, USA)
21 from 80-100 mg of frozen homogenised leaf tissue, followed by reverse transcription using High-
22 Capacity cDNA Reverse Transcription Kit (Thermo Fisher, USA). The expression of the target
23 and reference genes was analysed by RT-qPCR, as described previously (Petek et al., 2014;
24 Abdelhakim et al., 2021). QuantGenius (<http://quantgenius.nib.si>), was used for quality control,
25 standard curve-based relative gene expression quantification and imputation of values below level
26 of detection or quantification (LOD, LOQ) (Baebler et al., 2017).

27 Hormonomics

28 Concentration of the endogenous abscisate metabolites, auxin metabolites, jasmonates and
29 salicylic acid were determined in 10 mg of frozen homogenised leaf tissue according to the

1 method described (Flokova et al., 2014) and modified by Široká et al. (Siroka et al., 2022) (see
2 Supplementary methods for details). All experiments were repeated as four biological replicates.

3 Metabolomics

4 For determination of soluble sugar, starch and amino acid contents, 30 - 50 mg of freeze-dried
5 leaf or tuber material were extracted with 1 ml of 80% (v/v) ethanol. Soluble sugar and starch
6 content was determined as described in Hastilestari et al. (2018), while amino acids sample
7 preparation and measurements were performed as described elsewhere (Smith and Zeeman,
8 2006) (Obata et al., 2020).

9 Proteomics

10 High-throughput shotgun proteomics was done according to (Hoehenwarter et al., 2008) with
11 following modifications: 40 mg of leaf tissue from multiple stress conditions were freeze-dried in
12 liquid N₂ and ground using mortar and pestle. The proteins were extracted, pre-fractionated (40µg
13 of total protein were loaded onto the gel (1D SDS-PAGE), trypsin digested and desalted (using a
14 C18 spec plate) according to a previously described method (Chaturvedi et al., 2013; Ghatak et
15 al., 2016). One µg of purified peptides was loaded onto a C18 reverse-phase analytical column
16 (Thermo Scientific, EASY-Spray 50 cm, 2 µm particle size). Separation was achieved using a
17 two-and-a-half-hour gradient method, starting with a 4–35% buffer B (v/v) gradient [79.9% ACN,
18 0.1% formic acid (FA), 20% ultra-high purity water (MilliQ) over 90 minutes. Buffer A (v/v)
19 consisted of 0.1% FA in high-purity water (MilliQ). The flow rate was set to 300 nL/min. Mass
20 spectra were acquired in positive ion mode using a top-20 data-dependent acquisition (DDA)
21 method. A full MS scan was performed at 70,000 resolution (m/z 200) with a scan range of 380–
22 1800 m/z, followed by an MS/MS scan at 17,500 resolution (m/z 200). For MS/MS fragmentation,
23 higher energy collisional dissociation (HCD) was used with a normalized collision energy (NCE)
24 of 27%. Dynamic exclusion was set to 20 seconds.

25 Raw data were searched with the SEQUEST algorithm present in Proteome Discoverer version
26 1.3 (Thermo Scientific, Germany) described previously (Chaturvedi et al., 2015; Ghatak et al.,
27 2020). Pan-transcriptome (Petek et al., 2020) protein fasta was employed. The identified proteins
28 were quantitated based on total ion count and normalised using the normalised spectral
29 abundance factor (NSAF) strategy (Paoletti et al., 2006).

1 Data analysis

2 The programming environments R v.4.3 and v4.4 (<https://www.r-project.org/>) and Python v3.8
3 (www.python.org) were used. Experimentally acquired data is available from the Supplementary
4 Table 4. All data, code and algorithms, required for supporting, generating, or reproducing the
5 findings of this study are openly available in GitHub repository at [https://github.com/NIB-](https://github.com/NIB-SI/multiOmics-integration)
6 [SI/multiOmics-integration](https://github.com/NIB-SI/multiOmics-integration).

7 Data preprocessing

8 A master sample description metadata file was constructed (Supp. Table S1). Potential
9 inconsistencies between replicates were examined using pairwise plots between omics levels,
10 multidimensional scaling plots and scatterplot matrices within omics' levels using the vegan v2.6.-
11 4 R package (Oksanen et al., 2022). Missing values were handled as described in the
12 Supplementary methods. Due to many missing values, the neoPA (hormonomics) variable was
13 excluded from further analysis.

14 Variable selection was conducted on the non-invasive phenomics variable sets (Supp. Table S4).
15 The random forest (RF) algorithm from the R package caret v6.0-94 (Kuhn, 2008) as well as the
16 python package scikit-learn v1.2.0 were used with default settings, as RF showed the best
17 performance out of a selection of algorithms. Recursive feature elimination was applied in R and
18 multiple importance scores, including mutual information, Anova, RF importance and SHAP
19 values (Lundberg and Lee, 2017) were computed in Python, showing consistencies between the
20 approaches for the top 5 variables (top area, compactness, qL_Lss, ΔT , water consumption;
21 nonredundancy ranking in R). The sixth variable (F_v/F_m_Lss) was selected based on expert
22 knowledge.

23 Gene set enrichment was performed on the proteomics dataset using GSEA v4.3.2 (Subramanian
24 et al., 2005) and in-house generated gene sets (Supp. File S3, Supp. Table S6) and visualised
25 using biokit v0.1.1. Proteomics differential expression was conducted using the DEP v 1.22.0
26 package (Zhang et al., 2018) (Supp. Table S5). For downstream proteomics analyses,
27 differentially abundant and enriched proteins (from pathways important for this experimental
28 setup) were used. Waterlogging stress was cut-off at one-week duration, while triple stress (HDW)
29 was not considered in downstream analyses due to poor plant performance.

1 Analysis of individual omics data layers

2 Pearson correlation coefficient (PCC) heatmaps (pheatmap v1.0.12, heatmaply v. 1.5.0) were
3 generated within each treatment and for explicit treatment duration. Permutation-based t-test
4 (MKinfer v1.2) was used to denote differences between specific treatment and control within the
5 corresponding time-point (Kohl, 2024). Corresponding log₂FC were calculated. For downstream
6 analyses, 4 out of 6 replicates were chosen from non-invasive phenomics measurements to allow
7 integration with invasive phenomics and other omics measurements conducted on 4 replicates.

8 Integration across different omics datasets

9 Correlations between components measured in various Omics' levels were calculated and
10 visualised using DIABLO (Singh et al., 2019) as implemented in the mixOmics v6.24.0 package
11 (Rohart et al., 2017). The correlation matrix was calculated separately for each stress as well as
12 for control.

13 Integration of data with prior knowledge

14 A background knowledge network was manually constructed considering biochemical pathways
15 between measured variables. Where necessary, pathways were simplified to only include
16 representative variables, to prevent addition of many unmeasured nodes that would impede the
17 visualisation. Proteomics differential expression results were merged with t-test and log₂FC
18 results (Supp. Table S3). Final networks were visualised using DiNAR (Zagorscak et al., 2018)
19 and Cytoscape (Shannon et al., 2003).

20
21 For additional reports and some results not used in this manuscript see supplementary methods
22 and a project's GitHub repository <https://github.com/NIB-SI/multiOmics-integration>.

23
24
25
26
27
28
29
30
31

1 **Accession Numbers**

2 Links of gene names used in the study to GeneIDs can be found in Supplementary
3 table 5 for proteomics data and Supplementary table 7 for qPCR.

4 **Funding**

5 This work was funded by the EU H2020-SFS-2019-2 RIA project ADAPT, GA 2020 862-858 and
6 the Slovenian Research Agency (ARIS) under grant agreements P4-0165, J2-3060, and Z4-
7 50146. Moreover, this work was partially supported by the Ministry of Education, Youth and
8 Sports of the Czech Republic with the European Regional Development Fund-Project "SINGING
9 PLANT" (no. CZ.02.1.01/0.0/0.0/16_026/0008446).

10 **Acknowledgments**

11 The authors wish to thank Marijke Woudsma and Doretta Boomsma from HZPC Research for
12 providing the Désirée plantlets for this study and Mirella Sorrentino for help with conducting the
13 experiments at Photon Systems Instruments (PSI) Research Center (Drásov, Czech Republic).
14 Moreover, we thank following colleagues for their assistance and expertise: Stephen Reid
15 (FAU) and David Pscheidt (FAU) for measuring metabolite content, and Katja Stare (NIB) and
16 Nastja Marondini (NIB) for measuring gene expression.

17 **Author contributions**

18 KP, KG, SS, RS, CBa and MT conceptualized the study and designed the experiments, KP
19 measured phenotypic traits, ŠB measured gene expression, ON, AP and JŠ measured hormone
20 content, CS measured metabolite content, PC, AG prepared samples and performed proteomics
21 analysis, LAS performed LC-MS measurements for proteomics analysis; MZ curated data; MZ,
22 CB, AB, AZ and KG defined formal analysis methodology; MZ, CB, JZ, and AB conducted
23 statistical, mathematical and computational analysis; MZ, LA, NR, CB, AB, ŠB and KG performed
24 data visualisation; MZ, LA, NR, CB, SS, RS, KG, CBa and MT wrote the original draft. All authors
25 edited the manuscript and approved the final manuscript version. Detailed author contributions
26 are available from the Supp. Table S8.

1 Figure Legends

2 **Figure 1. Overview of the experimental design for single- and combined stress treatments and multi-**
 3 **omics sampling.** A) Summary of cultivation conditions. Timeline of the experimental set-up and applied
 4 stress treatments, including the recovery phase in potato cv. Désirée. Timing and duration of stress
 5 treatment and days for tissue sampling are shown. B) Actions comprised cultivation in the growing
 6 chambers and daily phenotyping with a set of sensors using the PlantScreen™ phenotyping platform at PSI
 7 Research Center. C) Automated image analysis pipeline was used to extract quantitative traits for
 8 morphological, physiological, and biochemical performance characterization of the plants during the stress
 9 treatment and recovery phase. Side view colour segmented RGB images of plants were digitally extracted
 10 for comparison at selected time points of tissue sampling (left panel) and daily plant volume (m^3) calculated
 11 from top and multiple angle side view RGB images (right panel). Black dotted lines reflect the initiation and
 12 removal of drought stress, respectively. Measurements, mean and standard error are shown ($n = 6$). C:
 13 control, D: individual drought stress, H: individual heat stress, HD: combined drought with heat stress, W:
 14 individual waterlogging stress, HDW: triple-stress condition.

15 **Figure 2. Physiological profiling using high-throughput phenotyping platforms reveals distinct**
 16 **responses to single and combined stresses.** A) Pixel-by-pixel false colour images of operating efficiency
 17 of photosystem II in light steady state (QY_{Lss} , arbitrary unit) captured by kinetic chlorophyll fluorescence
 18 measurement. Colour scale bar represents the range of fluorescence values. Images for selected time
 19 points of tissue sampling were digitally extracted for comparison. Colour coding of the treatments apply for
 20 the entire figure. Vertical dashed lines indicate the onset and end of drought. B) QY_{Lss} values extracted
 21 from images for each individual time point. C) Steady-state fluorescence of maximum efficiency of PSII
 22 photochemistry in the light trait based on chlorophyll fluorescence top view (F_v/F_m_{Lss}). D) steady-state
 23 estimation of the fraction of open reaction centres in PSII trait in light based on chlorophyll fluorescence top
 24 view (qL_{Lss}). E) Difference between canopy average temperature extracted from thermal IR images and
 25 air temperature measured in the thermal IR imaging unit (ΔT). F) Water use efficiency (WUE) based on
 26 plant volume and water consumption. A-F) Black dotted lines reflect the initiation and removal of drought
 27 stress, respectively. Measurements, mean and standard error are shown ($n = 6$). See Supplementary Table
 28 S3 for Statistical evaluation of differences between groups using Wilcoxon test. G) Tuber numbers counted
 29 per plant on the last day of the experiment (Day 28 = 60 days of cultivation). H) Harvest index calculated
 30 from the total biomass and tuber weight on the last day of the experiment. G-H) Measurements, mean and
 31 standard deviation are shown ($n = 4$). Statistical evaluation of differences between groups is given by the
 32 non-parametric Kruskal–Wallis test (*one-way ANOVA on ranks*); p-value above x-axis, where asterisk
 33 denotes p-value < 0.05. See Figure 1A for scheme on stress treatments. C: control, D: individual drought
 34 stress, H: individual heat stress, HD: combined drought with heat stress, W: individual waterlogging stress,
 35 HDW: triple-stress condition.

1
 2 **Figure 3: Integrated analysis of measured and generated data permits global visualization and multi-**
 3 **level amalgamation of potato stress responses.** A) Schematics of tissue sampling protocol. 2nd and 3rd
 4 leaves were harvested for destructive “omics” analysis, 4th leaf was used for relative water content
 5 calculation. Remaining plant tissue was quantified to obtain total above-ground biomass and tuber yield. B)
 6 Overview of data analysis pipeline. C) Dataset overview: multidimensional scaling shows combined HDW
 7 stressed plants as extremes, the centroid of each plant group is shown. D) Most informative variables from
 8 the phenomics level. Pearson correlation coefficients between them are presented as hierarchically
 9 clustered heat maps in waterlogging and heat stress. Abbreviations - Fv/Fm: Fv/Fm_Lss, qL: qL_Lss, top-
 10 area: top area, compact: compactness, water cons.: water consumption. For trait description see
 11 Supplementary Table S2.

12
 13 **Figure 4: Integration of multi-omics data in a knowledge-based metabolic and signaling network.** A)
 14 Structure of knowledge network. Individual studied components are coloured according to their function in
 15 different pathways. B) To compare the effects of different stresses on the overall state of the plant, we
 16 overlaid the knowledge networks with measured changes in component concentration. Nodes are coloured
 17 by log₂ fold changes (red – increase in stress compared to control, blue – decrease in stress compared to
 18 control, grey – measurement not available) shown for two time points: sampling day 8 and sampling day
 19 14 for the different stress treatments, days of stress treatment are given with each network (for more details
 20 of the set up see Figure 1A). Displayed omics measurements were obtained from leaf samples. Identifiers
 21 and descriptions corresponding to the short names shown in graphs are available in Supplementary Table
 22 S3 and Supplementary Table S5. ABA: Abscisic acid, Ca²⁺: Calcium, ET: Ethylene, HSP: Heat shock
 23 protein, IAA: Indole-3-acetic acid (Auxin), JA: Jasmonic acid, Pro: Proline, PS: Photosynthesis
 24 ROS: Reactive oxygen species, SA: Salicylic acid.

25
 26 **Figure 5: Combined heat and drought stress trigger distinct responses compared to each individual**
 27 **response.** Additive effect of combined stress is most pronounced for branched chain amino acids
 28 accumulation and JA signaling response. A-C) Heatmaps showing log₂FC (FDR p-value < 0.05) in
 29 individual stress heat (H) or drought (D) stress in comparison to combined one (HD) for targeted molecular
 30 analyses. Label colours indicate pathway associated with each molecule as in the Knowledge network (see
 31 Figure 4 for legend). A) Changes in metabolite levels. B) Changes in hormone levels, and C) Changes in
 32 selected stress-related transcripts. D) Changes observed on proteomics level. Results of Gene Set
 33 Enrichment Analysis (FDR q-value < 0.1) are shown. For more information see Supp. Table S6. E)
 34 Biochemical knowledge network showing changes under combined HD stress at day 14 (treatment day 7).
 35 In this version of knowledge network, only nodes that were significantly differentially expressed (vs. control
 36 conditions) are coloured and the connections between two differentially expressed nodes are coloured
 37 black. Node full black border indicates molecules with higher expression levels in HD compared to H and/or
 38 D alone. Dashed black border indicates molecules with lower expression levels in HD compared to H and/or

1 D alone (difference of $\log_2FC > 0.5$). Displayed omics measurements were obtained from leaf samples.
2 Identifiers and descriptions corresponding to the short names shown in graphs are available in
3 Supplementary Table S3 and Supplementary Table S5.

4
5 **Figure 6: Waterlogging triggers drought-stress like molecular responses in potato.** A-D) Heatmaps
6 showing \log_2FC (FDR p-value < 0.05) changes in A) metabolite levels, B) phytohormones, C) selected
7 stress-related transcripts. D) Volcano plot of differential proteomics analysis at day 7. Proteins with FDR p-
8 value < 0.05 shown as blue (downregulated) and red (upregulated) dots. For more information see Supp.
9 Table S5. E) Knowledge network of waterlogging stress at day 1 and day 7 (unfiltered, colour range [-2, 2]).
10 For legend see Figure 4. Displayed omics measurements were obtained from leaf samples. Identifiers and
11 descriptions corresponding to the short names shown in graphs are available in Supplementary Table S3
12 and Supplementary Table S5. D: individual drought stress, W: individual waterlogging stress.

13
14 **Figure 7. Schematic summary of multilevel responses to single and combined heat, drought and**
15 **waterlogging stresses.** Selected variables from each level are shown. Summary of molecular responses
16 (hormones, metabolites and transcripts) was based on the comparisons illustrated in Figures 5 and 6.
17 Summary of morphophysiological responses were based on the data from the last day of the experiment
18 (Day 28), which includes tuber information. Proteomics data set is not included here due to the small dataset
19 of differentially expressed proteins in the waterlogging treatment. Degree of increase or decrease is not
20 specified. ABA: Abscisic acid, DPA: Dihydrophaseic acid, Ja-Ile: Jasmonoyl-isoleucine, SP6A: SELF-
21 PRUNING 6A, HSP70: heat shock protein 70, RD29: Responsive to Desiccation 29B.

23 Competing interests

24 The authors declare no competing interests.

1 Data availability statement

2 Experimentally acquired data and data required to reproduce the analysis are available from
3 Supp. Table S4 and NIBs' GitHub repository <https://github.com/NIB-SI/multiOmics-integration>.

4 The MS/MS spectra of the identified proteins and their meta-information from both databases
5 have been deposited to the ProteomeXchange Consortium via the PRIDE partner repository
6 (<https://www.ebi.ac.uk/pride>) with the dataset identifier PXD052587.

7 References

- 8 **Abdelhakim LOA, Palma CFF, Zhou R, Wollenweber B, Ottosen CO, Rosenqvist E** (2021)
9 The effect of individual and combined drought and heat stress under elevated CO₂ on
10 physiological responses in spring wheat genotypes. *Plant Physiol Biochem* **162**: 301-314
- 11 **Abdelhakim LOA, Pleskacova B, Rodriguez-Granados NY, Sasidharan R, Perez-Borroto**
12 **LS, Sonnewald S, Gruden K, Vothknecht UC, Teige M, Panzarova K** (2024) High
13 Throughput Image-Based Phenotyping for Determining Morphological and Physiological
14 Responses to Single and Combined Stresses in Potato. *J Vis Exp*
- 15 **Abdelhakim LOA, Rosenqvist E, Wollenweber B, Spyroglou I, Ottosen C-O, Panzarová K**
16 (2021) Investigating Combined Drought- and Heat Stress Effects in Wheat under
17 Controlled Conditions by Dynamic Image-Based Phenotyping. *Agronomy* **11**: 364
- 18 **Abelenda JA, Bergonzi S, Oortwijn M, Sonnewald S, Du M, Visser RGF, Sonnewald U,**
19 **Bachem CWB** (2019) Source-Sink Regulation Is Mediated by Interaction of an FT
20 Homolog with a SWEET Protein in Potato. *Curr Biol* **29**: 1178-1186 e1176
- 21 **Abelenda JA, Cruz-Oro E, Franco-Zorrilla JM, Prat S** (2016) Potato StCONSTANS-like1
22 Suppresses Storage Organ Formation by Directly Activating the FT-like StSP5G
23 Repressor. *Curr Biol* **26**: 872-881
- 24 **Akbudak MA, Yildiz S, Filiz E** (2020) Pathogenesis related protein-1 (PR-1) genes in tomato
25 (*Solanum lycopersicum* L.): Bioinformatics analyses and expression profiles in response
26 to drought stress. *Genomics* **112**: 4089-4099
- 27 **Awlia M, Nigro A, Fajkus J, Schmoeckel SM, Negrao S, Santelia D, Trtilek M, Tester M,**
28 **Julkowska MM, Panzarova K** (2016) High-Throughput Non-destructive Phenotyping of
29 Traits that Contribute to Salinity Tolerance in *Arabidopsis thaliana*. *Front Plant Sci* **7**:
30 1414
- 31 **Bachmann A, Hause B, Maucher H, Garbe E, Voros K, Weichert H, Wasternack C,**
32 **Feussner I** (2002) Jasmonate-induced lipid peroxidation in barley leaves initiated by
33 distinct 13-LOX forms of chloroplasts. *Biol Chem* **383**: 1645-1657
- 34 **Baebler S, Svalina M, Petek M, Stare K, Rotter A, Pompe-Novak M, Gruden K** (2017)
35 quantGenius: implementation of a decision support system for qPCR-based gene
36 quantification. *BMC Bioinformatics* **18**: 276
- 37 **Bailey-Serres J, Parker JE, Ainsworth EA, Oldroyd GED, Schroeder JI** (2019) Genetic
38 strategies for improving crop yields. *Nature* **575**: 109-118
- 39 **Balfagon D, Sengupta S, Gomez-Cadenas A, Fritschi FB, Azad RK, Mittler R, Zandalinas**
40 **SI** (2019) Jasmonic Acid Is Required for Plant Acclimation to a Combination of High
41 Light and Heat Stress. *Plant Physiol* **181**: 1668-1682

- 1 **Benitez-Alfonso Y, Soanes BK, Zimba S, Sinanaj B, German L, Sharma V, Bohra A,**
2 **Kolesnikova A, Dunn JA, Martin AC, Khashi URM, Saati-Santamaria Z, Garcia-**
3 **Fraile P, Ferreira EA, Frazao LA, Cowling WA, Siddique KHM, Pandey MK, Farooq**
4 **M, Varshney RK, Chapman MA, Boesch C, Daszkowska-Golec A, Foyer CH (2023)**
5 **Enhancing climate change resilience in agricultural crops. *Curr Biol* 33: R1246-R1261**
6 **Bittner A, Ciesla A, Gruden K, Lukan T, Mahmud S, Teige M, Vothknecht UC, Wurzinger B**
7 **(2022) Organelles and phytohormones: a network of interactions in plant stress**
8 **responses. *J Exp Bot* 73: 7165-7181**
9 **Bleker C, Ramsak Z, Bittner A, Podpecan V, Zagorscak M, Wurzinger B, Baebler S, Petek**
10 **M, Kriznik M, van Dieren A, Gruber J, Afjehi-Sadat L, Weckwerth W, Zupanic A,**
11 **Teige M, Vothknecht UC, Gruden K (2024) Stress Knowledge Map: A knowledge**
12 **graph resource for systems biology analysis of plant stress responses. *Plant Commun:***
13 **100920**
14 **Cembrowska-Lech D, Krzeminska A, Miller T, Nowakowska A, Adamski C, Radaczynska**
15 **M, Mikiciuk G, Mikiciuk M (2023) An Integrated Multi-Omics and Artificial Intelligence**
16 **Framework for Advance Plant Phenotyping in Horticulture. *Biology (Basel)* 12**
17 **Chaturvedi P, Doerfler H, Jegadeesan S, Ghatak A, Pressman E, Castillejo MA, Wienkoop**
18 **S, Egelhofer V, Firon N, Weckwerth W (2015) Heat-Treatment-Responsive Proteins in**
19 **Different Developmental Stages of Tomato Pollen Detected by Targeted Mass Accuracy**
20 **Precursor Alignment (tMAPA). *J Proteome Res* 14: 4463-4471**
21 **Chaturvedi P, Ischebeck T, Egelhofer V, Lichtscheidl I, Weckwerth W (2013) Cell-specific**
22 **analysis of the tomato pollen proteome from pollen mother cell to mature pollen provides**
23 **evidence for developmental priming. *J Proteome Res* 12: 4892-4903**
24 **Chen Q, Hu T, Li X, Song CP, Zhu JK, Chen L, Zhao Y (2022) Phosphorylation of SWEET**
25 **sucrose transporters regulates plant root:shoot ratio under drought. *Nat Plants* 8: 68-77**
26 **Clarke SM, Cristescu SM, Miersch O, Harren FJM, Wasternack C, Mur LAJ (2009)**
27 **Jasmonates act with salicylic acid to confer basal thermotolerance in *Arabidopsis***
28 ***thaliana*. *New Phytol* 182: 175-187**
29 **Cutler SR, Rodriguez PL, Finkelstein RR, Abrams SR (2010) Abscisic acid: emergence of a**
30 **core signaling network. *Annu Rev Plant Biol* 61: 651-679**
31 **Dahal K, Li XQ, Tai H, Creelman A, Bizimungu B (2019) Improving Potato Stress Tolerance**
32 **and Tuber Yield Under a Climate Change Scenario - A Current Overview. *Front Plant***
33 ***Sci* 10: 563**
34 **Demirel U, Morris WL, Ducreux LJM, Yavuz C, Asim A, Tindas I, Campbell R, Morris JA,**
35 **Verrall SR, Hedley PE, Gokce ZNO, Caliskan S, Aksoy E, Caliskan ME, Taylor MA,**
36 **Hancock RD (2020) Physiological, Biochemical, and Transcriptional Responses to**
37 **Single and Combined Abiotic Stress in Stress-Tolerant and Stress-Sensitive Potato**
38 **Genotypes. *Front Plant Sci* 11: 169**
39 **FAO (2023) The Impact of Disasters on Agriculture and Food Security 2023 – Avoiding and**
40 **reducing losses through investment in resilience. . *In*. FAO, Rome, Italy, p #168 p.**
41 **Findurová H, Veselá B, Panzarová K, Pytela J, Trtílek M, Klem K (2023) Phenotyping**
42 **drought tolerance and yield performance of barley using a combination of imaging**
43 **methods. *Environmental and Experimental Botany* 209: 105314**
44 **Flokova K, Tarkowska D, Miersch O, Strnad M, Wasternack C, Novak O (2014) UHPLC-**
45 **MS/MS based target profiling of stress-induced phytohormones. *Phytochemistry* 105:**
46 **147-157**
47 **Gautam T, Dutta M, Jaiswal V, Zinta G, Gahlaut V, Kumar S (2022) Emerging Roles of**
48 **SWEET Sugar Transporters in Plant Development and Abiotic Stress Responses. *Cells***
49 **11**
50 **Geldhof B, Pattyn J, Van de Poel B (2023) From a different angle: genetic diversity underlies**
51 **differentiation of waterlogging-induced epinasty in tomato. *Front Plant Sci* 14: 1178778**

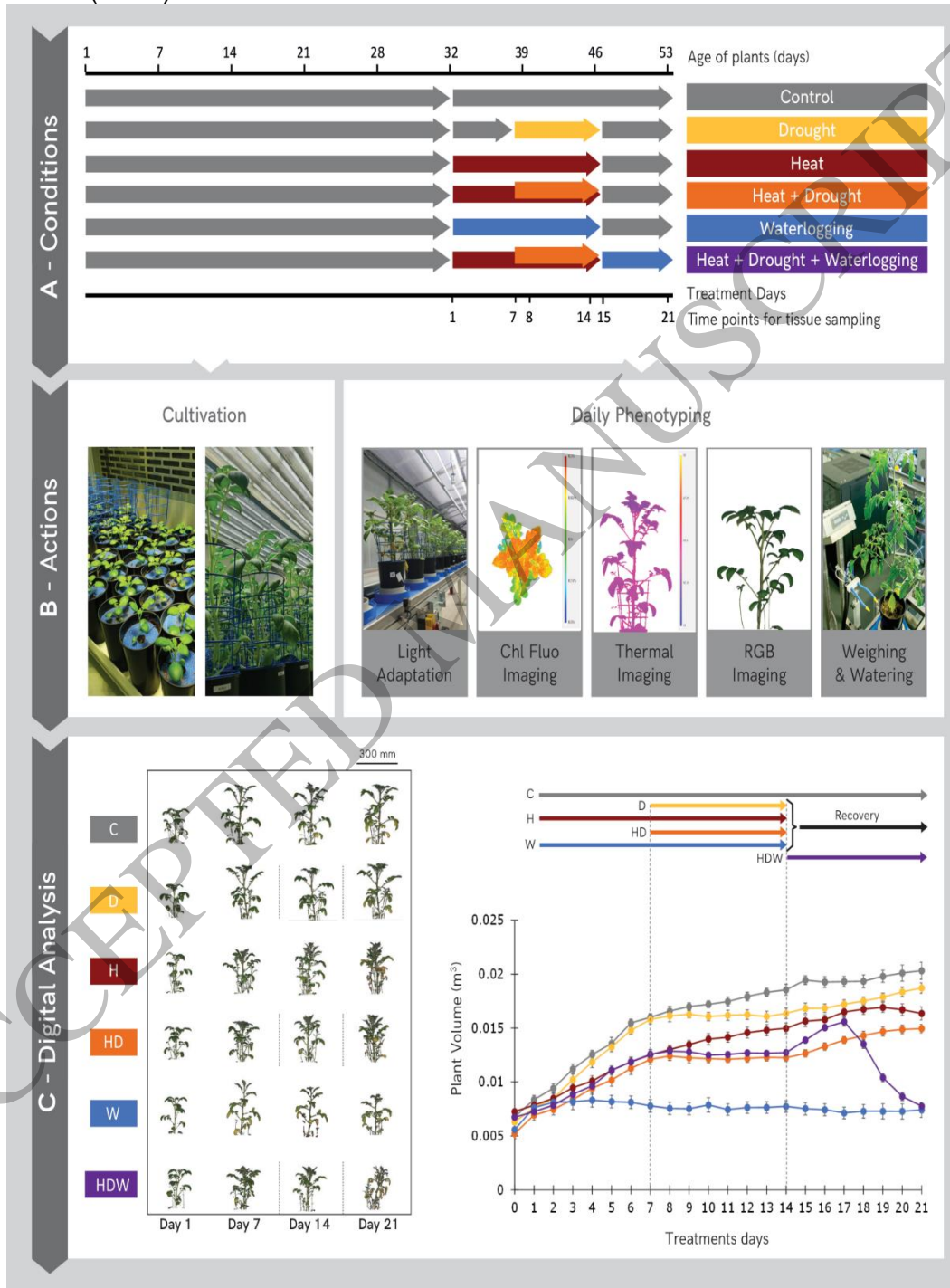
- 1 **Ghatak A, Chaturvedi P, Bachmann G, Valledor L, Ramsak Z, Bazargani MM, Bajaj P,**
2 **Jegadeesan S, Li W, Sun X, Gruden K, Varshney RK, Weckwerth W** (2020)
3 Physiological and Proteomic Signatures Reveal Mechanisms of Superior Drought
4 Resilience in Pearl Millet Compared to Wheat. *Front Plant Sci* **11**: 600278
- 5 **Ghatak A, Chaturvedi P, Nagler M, Roustan V, Lyon D, Bachmann G, Postl W, Schrofl A,**
6 **Desai N, Varshney RK, Weckwerth W** (2016) Comprehensive tissue-specific proteome
7 analysis of drought stress responses in *Pennisetum glaucum* (L.) R. Br. (Pearl millet). *J*
8 *Proteomics* **143**: 122-135
- 9 **Grieco M, Roustan V, Dermendjiev G, Rantala S, Jain A, Leonardelli M, Neumann K,**
10 **Berger V, Engelmeier D, Bachmann G, Ebersberger I, Aro EM, Weckwerth W, Teige**
11 **M** (2020) Adjustment of photosynthetic activity to drought and fluctuating light in wheat.
12 *Plant Cell Environ* **43**: 1484-1500
- 13 **Guihur A, Rebeaud ME, Goloubinoff P** (2022) How do plants feel the heat and survive?
14 *Trends Biochem Sci* **47**: 824-838
- 15 **Hall RD, D'Auria JC, Silva Ferreira AC, Gibon Y, Kruszka D, Mishra P, van de Zedde R**
16 (2022) High-throughput plant phenotyping: a role for metabolomics? *Trends Plant Sci*
17 **27**: 549-563
- 18 **Hancock RD, Morris WL, Ducreux LJ, Morris JA, Usman M, Verrall SR, Fuller J, Simpson**
19 **CG, Zhang R, Hedley PE, Taylor MA** (2014) Physiological, biochemical and molecular
20 responses of the potato (*Solanum tuberosum* L.) plant to moderately elevated
21 temperature. *Plant Cell Environ* **37**: 439-450
- 22 **Hastilestari BR, Lorenz J, Reid S, Hofmann J, Pscheidt D, Sonnewald U, Sonnewald S**
23 (2018) Deciphering source and sink responses of potato plants (*Solanum tuberosum* L.)
24 to elevated temperatures. *Plant Cell Environ* **41**: 2600-2616
- 25 **Hoehenwarter W, van Dongen JT, Wienkoop S, Steinfath M, Hummel J, Erban A, Sulpice**
26 **R, Regierer B, Kopka J, Geigenberger P, Weckwerth W** (2008) A rapid approach for
27 phenotype-screening and database independent detection of cSNP/protein
28 polymorphism using mass accuracy precursor alignment. *Proteomics* **8**: 4214-4225
- 29 **Jackson MB, Campbell DJ** (1976) Waterlogging and petiole epinasty in tomato: The role of
30 ethylene and low oxygen. *New Phytologist* **76**: 21-29
- 31 **Jackson MB, Hall KC** (1987) Early stomatal closure in waterlogged pea plants is mediated by
32 abscisic acid in the absence of foliar water deficits. *Plant, Cell & Environment* **10**: 121-
33 130
- 34 **Jamil IN, Remali J, Azizan KA, Nor Muhammad NA, Arita M, Goh HH, Aizat WM** (2020)
35 Systematic Multi-Omics Integration (MOI) Approach in Plant Systems Biology. *Front*
36 *Plant Sci* **11**: 944
- 37 **Joshi S, Patil S, Shaikh A, Jamla M, Kumar V** (2024) Modern omics toolbox for producing
38 combined and multifactorial abiotic stress tolerant plants. *Plant Stress* **11**: 100301
- 39 **Jovović Z, Bročić A, Velimirović ŽD, A. Komnenić** (2021) The influence of flooding on the
40 main parameters of potato productivity. *In*, Ed 1320. International Society for
41 Horticultural Science (ISHS), Leuven, Belgium, pp 133-138
- 42 **Kanehisa M, Furumichi M, Tanabe M, Sato Y, Morishima K** (2017) KEGG: new perspectives
43 on genomes, pathways, diseases and drugs. *Nucleic Acids Res* **45**: D353-D361
- 44 **Koch L, Lehretz GG, Sonnewald U, Sonnewald S** (2024) Yield reduction caused by elevated
45 temperatures and high nitrogen fertilization is mitigated by SP6A overexpression in
46 potato (*Solanum tuberosum* L.). *Plant J* **117**: 1702-1715
- 47 **Kromdijk J, Glowacka K, Leonelli L, Gabilly ST, Iwai M, Niyogi KK, Long SP** (2016)
48 Improving photosynthesis and crop productivity by accelerating recovery from
49 photoprotection. *Science* **354**: 857-861
- 50 **Lal MK, Tiwari RK, Kumar A, Dey A, Kumar R, Kumar D, Jaiswal A, Changan SS, Raigond**
51 **P, Dutt S, Luthra SK, Mandal S, Singh MP, Paul V, Singh B** (2022) Mechanistic

- 1 Concept of Physiological, Biochemical, and Molecular Responses of the Potato Crop to
2 Heat and Drought Stress. *Plants (Basel)* **11**
- 3 **Lee AH, Shannon CP, Amenyogbe N, Bennike TB, Diray-Arce J, Idoko OT, Gill EE, Ben-**
4 **Othman R, Pomat WS, van Haren SD, Cao KL, Cox M, Darboe A, Falsafi R, Ferrari**
5 **D, Harbeson DJ, He D, Bing C, Hinshaw SJ, Ndure J, Njie-Jobe J, Pettengill MA,**
6 **Richmond PC, Ford R, Saleu G, Masiria G, Matlam JP, Kirarock W, Roberts E,**
7 **Malek M, Sanchez-Schmitz G, Singh A, Angelidou A, Smolen KK, Consortium E,**
8 **Brinkman RR, Ozonoff A, Hancock REW, van den Biggelaar AHJ, Steen H, Tebbutt**
9 **SJ, Kampmann B, Levy O, Kollmann TR** (2019) Dynamic molecular changes during
10 the first week of human life follow a robust developmental trajectory. *Nat Commun* **10**:
11 1092
- 12 **Leeggangers HACF, Rodriguez-Granados NY, Macias-Honti MG, Sasidharan R** (2023) A
13 helping hand when drowning: The versatile role of ethylene in root flooding resilience.
14 *Environmental and Experimental Botany* **213**: 105422
- 15 **Lehretz GG, Sonnewald S, Lugassi N, Granot D, Sonnewald U** (2020) Future-Proofing
16 Potato for Drought and Heat Tolerance by Overexpression of Hexokinase and SP6A.
17 *Front Plant Sci* **11**: 614534
- 18 **Li B, Zeng Y, Cao W, Zhang W, Cheng L, Yin H, Wu Q, Wang X, Huang Y, Lau WCY, Yao**
19 **ZP, Guo Y, Jiang L** (2021) A distinct giant coat protein complex II vesicle population in
20 *Arabidopsis thaliana*. *Nat Plants* **7**: 1335-1346
- 21 **Liu T, Salguero P, Petek M, Martinez-Mira C, Balzano-Nogueira L, Ramsak Z, McIntyre L,**
22 **Gruden K, Tarazona S, Conesa A** (2022) PaintOmics 4: new tools for the integrative
23 analysis of multi-omics datasets supported by multiple pathway databases. *Nucleic*
24 *Acids Res* **50**: W551-W559
- 25 **Lothier J, Diab H, Cukier C, Limami AM, Tcherkez G** (2020) Metabolic Responses to
26 Waterlogging Differ between Roots and Shoots and Reflect Phloem Transport Alteration
27 in *Medicago truncatula*. *Plants (Basel)* **9**
- 28 **Lozano-Elena F, Fàbregas N, Coletto-Alcudia V, Caño-Delgado AI** (2022) Analysis of
29 metabolic dynamics during drought stress in *Arabidopsis* plants. *Scientific Data* **9**: 90
- 30 **Lozano-Juste J, Cutler SR** (2016) Hormone signalling: ABA has a breakdown. *Nat Plants* **2**:
31 16137
- 32 **Lundberg SM, Lee S-I** (2017) A unified approach to interpreting model predictions. *In*
33 *Proceedings of the 31st International Conference on Neural Information Processing*
34 *Systems*. Curran Associates Inc., Long Beach, California, USA, pp 4768–4777
- 35 **Mahmud S, Ullah C, Kortz A, Bhattacharyya S, Yu P, Gershenzon J, Vothknecht UC** (2022)
36 Constitutive expression of JASMONATE RESISTANT 1 induces molecular changes that
37 prime the plants to better withstand drought. *Plant Cell Environ* **45**: 2906-2922
- 38 **Manjunath KK, Krishna H, Devate NB, Sunilkumar VP, Patil SP, Chauhan D, Singh S,**
39 **Kumar S, Jain N, Singh GP, Singh PK** (2023) QTL mapping: insights into genomic
40 regions governing component traits of yield under combined heat and drought stress in
41 wheat. *Front Genet* **14**: 1282240
- 42 **Mathur S, Agrawal D, Jajoo A** (2014) Photosynthesis: Response to high temperature stress.
43 *Journal of Photochemistry and Photobiology B: Biology* **137**: 116-126
- 44 **Mishra S, Srivastava AK, Khan AW, Tran LP, Nguyen HT** (2024) The era of panomics-driven
45 gene discovery in plants. *Trends Plant Sci*
- 46 **Mittler R** (2006) Abiotic stress, the field environment and stress combination. *Trends Plant Sci*
47 **11**: 15-19
- 48 **Nakamura Y, Mithofer A, Kombrink E, Boland W, Hamamoto S, Uozumi N, Tohma K, Ueda**
49 **M** (2011) 12-hydroxyjasmonic acid glucoside is a COI1-JAZ-independent activator of
50 leaf-closing movement in *Samanea saman*. *Plant Physiol* **155**: 1226-1236

- 1 **Navarro C, Abelenda JA, Cruz-Oro E, Cuellar CA, Tamaki S, Silva J, Shimamoto K, Prat S**
2 (2011) Control of flowering and storage organ formation in potato by FLOWERING
3 LOCUS T. *Nature* **478**: 119-122
- 4 **Núñez-Lillo G, Ponce E, Arancibia-Guerra C, Carpentier S, Carrasco-Pancorbo A, Olmo-**
5 **García L, Chirinos R, Campos D, Campos-Vargas R, Meneses C, Pedreschi R**
6 (2023) A multiomics integrative analysis of color de-synchronization with softening of
7 'Hass' avocado fruit: A first insight into a complex physiological disorder. *Food Chemistry*
8 **408**: 135215
- 9 **Núñez-Lillo G, Ponce E, Beyer CP, Álvaro JE, Meneses C, Pedreschi R** (2024) A First
10 Omics Data Integration Approach in Hass Avocados to Evaluate Rootstock–Scion
11 Interactions: From Aerial and Root Plant Growth to Fruit Development. *Plants* **13**: 603
- 12 **Obata T, Klemens PAW, Rosado-Souza L, Schlereth A, Gisel A, Stavolone L, Zierer W,**
13 **Morales N, Mueller LA, Zeeman SC, Ludewig F, Stitt M, Sonnewald U, Neuhaus HE,**
14 **Fernie AR** (2020) Metabolic profiles of six African cultivars of cassava (*Manihot*
15 *esculenta* Crantz) highlight bottlenecks of root yield. *Plant J* **102**: 1202-1219
- 16 **Paoletti AC, Parmely TJ, Tomomori-Sato C, Sato S, Zhu D, Conaway RC, Conaway JW,**
17 **Florens L, Washburn MP** (2006) Quantitative proteomic analysis of distinct mammalian
18 Mediator complexes using normalized spectral abundance factors. *Proc Natl Acad Sci U*
19 *S A* **103**: 18928-18933
- 20 **Park JS, Park SJ, Kwon SY, Shin AY, Moon KB, Park JM, Cho HS, Park SU, Jeon JH, Kim**
21 **HS, Lee HJ** (2022) Temporally distinct regulatory pathways coordinate thermo-
22 responsive storage organ formation in potato. *Cell Rep* **38**: 110579
- 23 **Petek M, Rotter A, Kogovsek P, Baebler S, Mithofer A, Gruden K** (2014) Potato virus Y
24 infection hinders potato defence response and renders plants more vulnerable to
25 Colorado potato beetle attack. *Mol Ecol* **23**: 5378-5391
- 26 **Petek M, Zagorscak M, Ramsak Z, Sanders S, Tomaz S, Tseng E, Zouine M, Coll A,**
27 **Gruden K** (2020) Cultivar-specific transcriptome and pan-transcriptome reconstruction
28 of tetraploid potato. *Sci Data* **7**: 249
- 29 **Ployet R, Veneziano Labate MT, Regiani Cataldi T, Christina M, Morel M, San Clemente H,**
30 **Denis M, Favreau B, Tomazello Filho M, Laclau J-P, Labate CA, Chaix G, Grima-**
31 **Pettenati J, Mounet F** (2019) A systems biology view of wood formation in *Eucalyptus*
32 *grandis* trees submitted to different potassium and water regimes. *New Phytologist* **223**:
33 766-782
- 34 **Quint M, Delker C, Franklin KA, Wigge PA, Halliday KJ, van Zanten M** (2016) Molecular and
35 genetic control of plant thermomorphogenesis. *Nat Plants* **2**: 15190
- 36 **Renziehausen T, Frings S, Schmidt-Schippers R** (2024) 'Against all floods': plant adaptation
37 to flooding stress and combined abiotic stresses. *Plant J*
- 38 **Rivero RM, Mittler R, Blumwald E, Zandalinas SI** (2022) Developing climate-resilient crops:
39 improving plant tolerance to stress combination. *Plant J* **109**: 373-389
- 40 **Rohart F, Gautier B, Singh A, Le Cao KA** (2017) mixOmics: An R package for 'omics feature
41 selection and multiple data integration. *PLoS Comput Biol* **13**: e1005752
- 42 **Sato H, Mizoi J, Shinozaki K, Yamaguchi-Shinozaki K** (2024) Complex plant responses to
43 drought and heat stress under climate change. *Plant J*
- 44 **Sauter M** (2013) Root responses to flooding. *Curr Opin Plant Biol* **16**: 282-286
- 45 **Singh A, Shannon CP, Gautier B, Rohart F, Vacher M, Tebbutt SJ, Lê Cao K-A** (2019)
46 DIABLO: an integrative approach for identifying key molecular drivers from multi-omics
47 assays. *Bioinformatics* **35**: 3055-3062
- 48 **Sinha R, Pelaez-Vico MA, Shostak B, Nguyen TT, Pascual LS, Ogdén AM, Lyu Z,**
49 **Zandalinas SI, Joshi T, Fritschi FB, Mittler R** (2024) The effects of multifactorial stress
50 combination on rice and maize. *Plant Physiol* **194**: 1358-1369

- 1 **Siroka J, Brunoni F, Pencik A, Mik V, Zukauskaitė A, Strnad M, Novak O, Flokova K** (2022)
2 High-throughput interspecies profiling of acidic plant hormones using miniaturised
3 sample processing. *Plant Methods* **18**: 122
- 4 **Smith AM, Zeeman SC** (2006) Quantification of starch in plant tissues. *Nat Protoc* **1**: 1342-
5 1345
- 6 **Stael S, Kmieciak P, Willems P, Van Der Kelen K, Coll NS, Teige M, Van Breusegem F**
7 (2015) Plant innate immunity--sunny side up? *Trends Plant Sci* **20**: 3-11
- 8 **Tang R, Niu S, Zhang G, Chen G, Haroon M, Yang Q, Rajora OP, Li X-Q** (2018)
9 Physiological and growth responses of potato cultivars to heat stress. *Botany* **96**: 897-
10 912
- 11 **Trapero-Mozos A, Morris WL, Ducreux LJM, McLean K, Stephens J, Torrance L, Bryan**
12 **GJ, Hancock RD, Taylor MA** (2018) Engineering heat tolerance in potato by
13 temperature-dependent expression of a specific allele of HEAT-SHOCK COGNATE 70.
14 *Plant Biotechnol J* **16**: 197-207
- 15 **von Gehren P, Bomers S, Tripolt T, Söllinger J, Prat N, Redondo B, Vorss R, Teige M,**
16 **Kamptner A, Ribarits A** (2023) Farmers Feel the Climate Change: Variety Choice as an
17 Adaptation Strategy of European Potato Farmers. *Climate* **11**: 189
- 18 **Wasternack C, Feussner I** (2018) The Oxylinin Pathways: Biochemistry and Function. *Annu*
19 *Rev Plant Biol* **69**: 363-386
- 20 **Weckwerth W, Ghatak A, Bellaire A, Chaturvedi P, Varshney RK** (2020) PANOMICS meets
21 germplasm. *Plant Biotechnol J* **18**: 1507-1525
- 22 **Weng JK, Ye M, Li B, Noel JP** (2016) Co-evolution of Hormone Metabolism and Signaling
23 Networks Expands Plant Adaptive Plasticity. *Cell* **166**: 881-893
- 24 **Wu Q, Su N, Huang X, Cui J, Shabala L, Zhou M, Yu M, Shabala S** (2021) Hypoxia-induced
25 increase in GABA content is essential for restoration of membrane potential and
26 preventing ROS-induced disturbance to ion homeostasis. *Plant Commun* **2**: 100188
- 27 **Yang W, Feng H, Zhang X, Zhang J, Doonan JH, Batchelor WD, Xiong L, Yan J** (2020) Crop
28 Phenomics and High-Throughput Phenotyping: Past Decades, Current Challenges, and
29 Future Perspectives. *Mol Plant* **13**: 187-214
- 30 **Yoshida T, Fernie AR** (2024) Hormonal regulation of plant primary metabolism under drought.
31 *J Exp Bot* **75**: 1714-1725
- 32 **Yoshihara T, Omir E-SA, Koshino H, Sakamura S, Kkuta Y, Koda Y** (1989) Structure of a
33 Tuber-inducing Stimulus from Potato Leaves (*Solanum tuberosum* L.). *Agricultural and*
34 *Biological Chemistry* **53**: 2835-2837
- 35 **Zaki HEM, Radwan KSA** (2022) Response of potato (*Solanum tuberosum* L.) cultivars to
36 drought stress under in vitro and field conditions. *Chemical and Biological Technologies*
37 *in Agriculture* **9**: 1
- 38 **Zandalinas SI, Fritschi FB, Mittler R** (2021) Global Warming, Climate Change, and
39 Environmental Pollution: Recipe for a Multifactorial Stress Combination Disaster. *Trends*
40 *Plant Sci* **26**: 588-599
- 41 **Zandalinas SI, Pelaez-Vico MA, Sinha R, Pascual LS, Mittler R** (2023) The impact of
42 multifactorial stress combination on plants, crops, and ecosystems: how should we
43 prepare for what comes next? *Plant J*
- 44 **Zeng ZL, Wang XQ, Zhang SB, Huang W** (2024) Mesophyll conductance limits photosynthesis
45 in fluctuating light under combined drought and heat stresses. *Plant Physiol* **194**: 1498-
46 1511
- 47 **Zhang H, Sonnewald U** (2017) Differences and commonalities of plant responses to single and
48 combined stresses. *Plant J* **90**: 839-855
- 49 **Zhang H, Zhu J, Gong Z, Zhu JK** (2022) Abiotic stress responses in plants. *Nat Rev Genet* **23**:
50 104-119

- 1 **Zhang R, Zhang C, Yu C, Dong J, Hu J (2022)** Integration of multi-omics technologies for crop
 2 improvement: Status and prospects. *Front Bioinform* **2**: 1027457
 3 **Zhao Y, Zhang W, Abou-Elwafa SF, Shabala S, Xu L (2021)** Understanding a Mechanistic
 4 Basis of ABA Involvement in Plant Adaptation to Soil Flooding: The Current Standing.
 5 *Plants (Basel)* **10**



6
7
8

Figure 1
210x235 mm (x DPI)

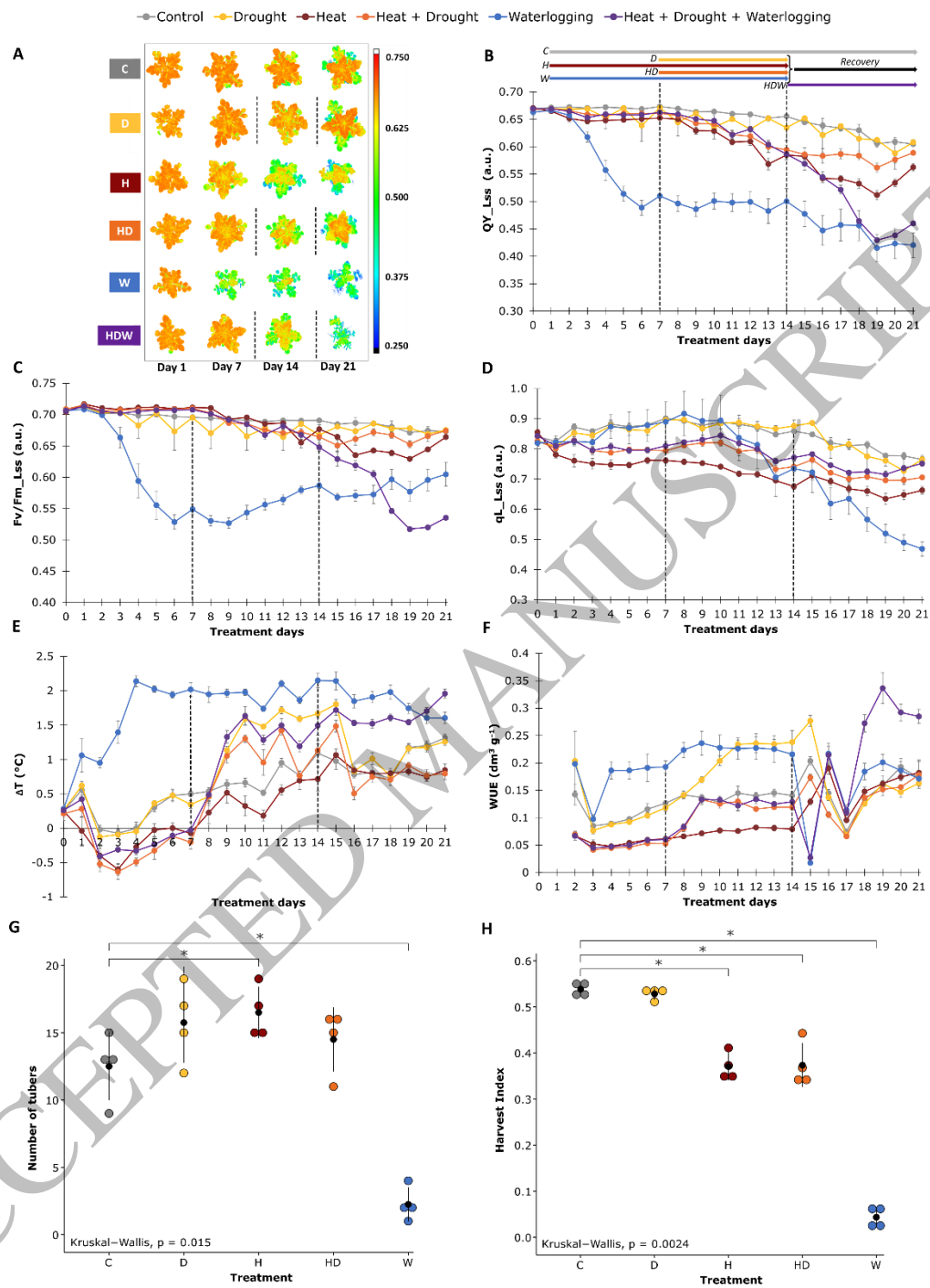


Figure 2
419x559 mm (x DPI)

1
2
3
4

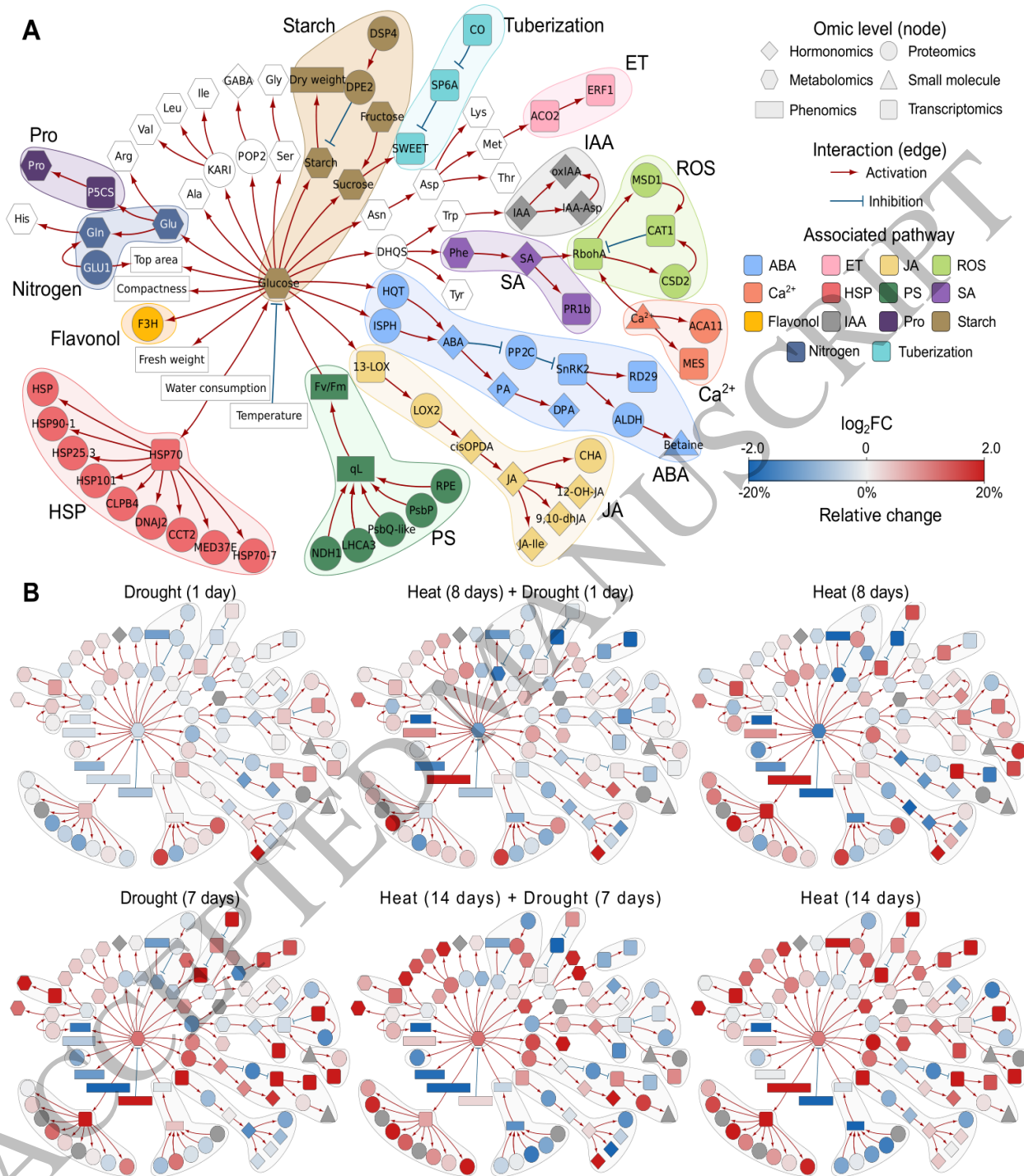


Figure 4
193x204 mm (x DPI)

1
2
3
4

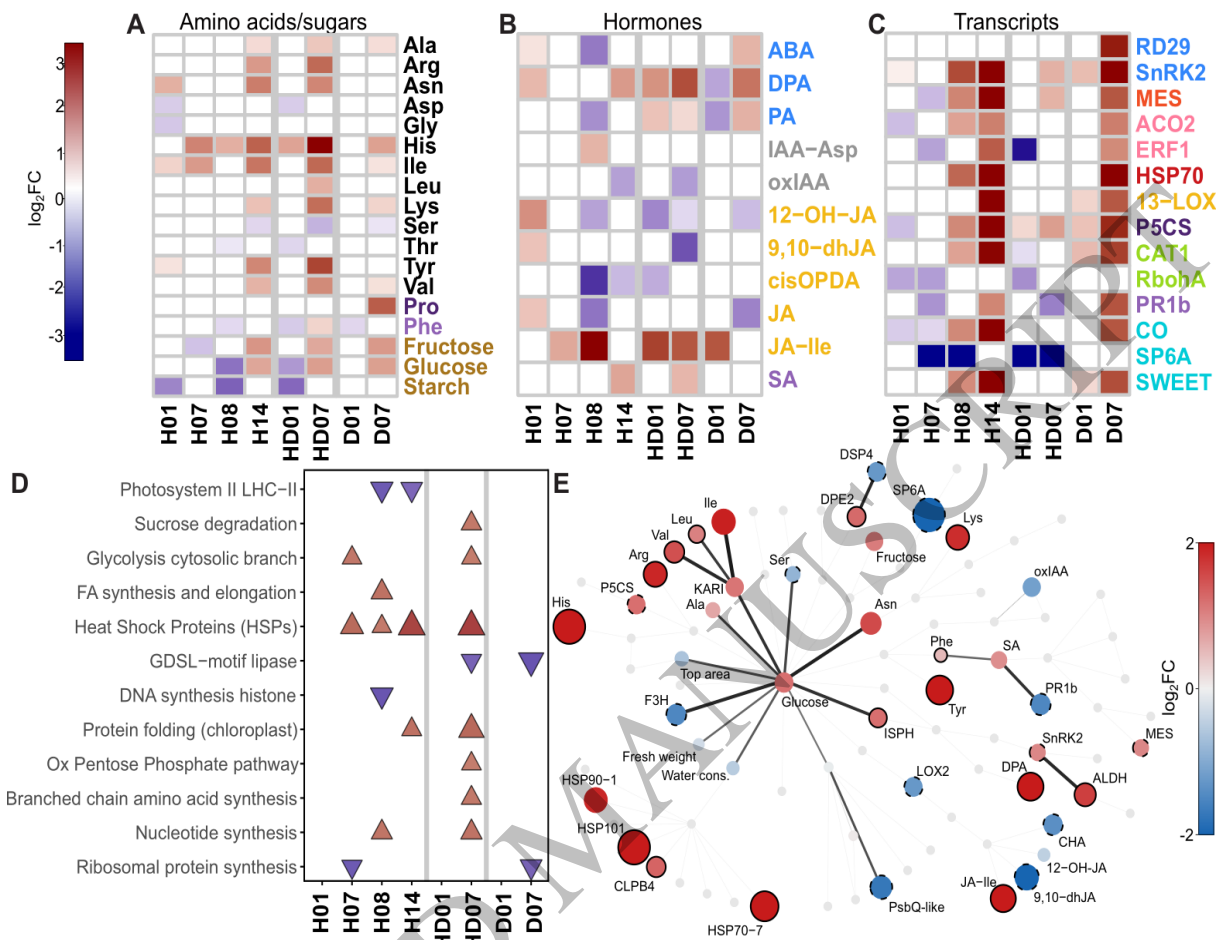


Figure 5
198x150 mm (x DPI)

1
2
3
4

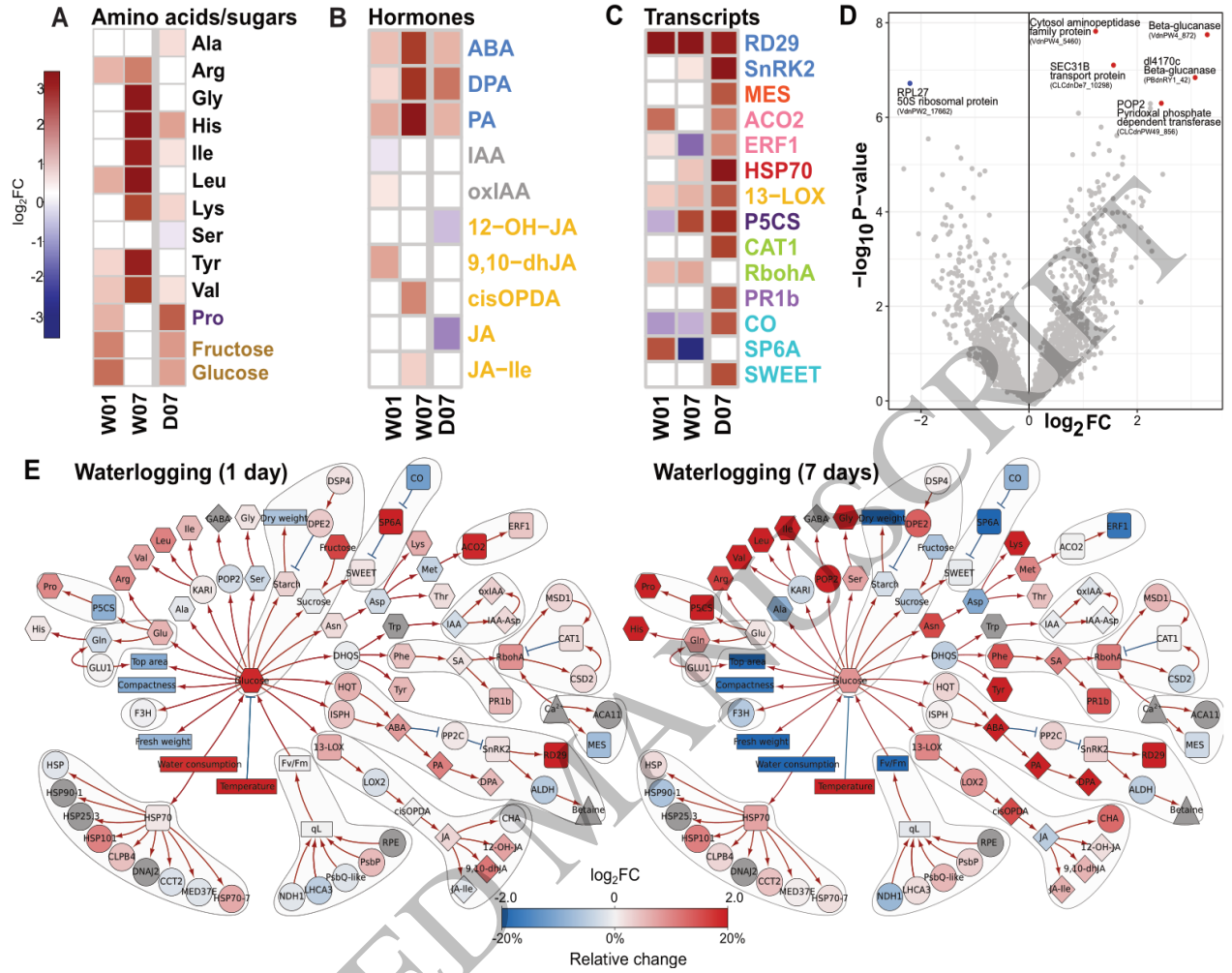
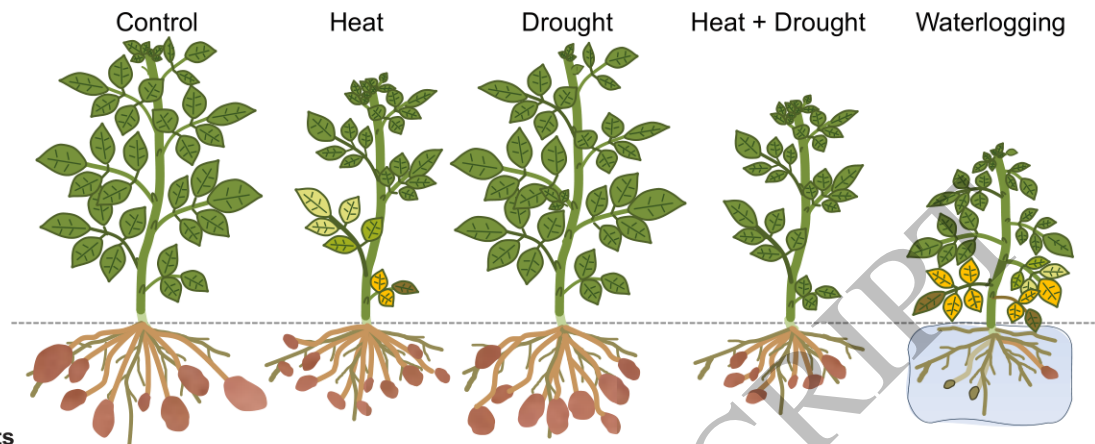


Figure 6
198x150 mm (x DPI)

1
2
3
4



Phenotypic traits	Control	Heat	Drought	Heat + Drought	Waterlogging
Plant volume		↓	↓	↓	↓
Photosynthesis		↓	↓	↓	↓
Leaf temperature		↓	↑	●	↑
Tuber FW		↓	●	↓	↓
Tuber number		↑	●	●	↓
Hormones & derivatives					
ABA		↓	↑	●	↑
DPA		↑	↑	↑	↑
JA-Ile		↑	●	↑	↑
Metabolites					
Histidine		↑	↑	↑	↑
Glucose		↑	↑	↑	●
Proline		●	↑	●	↑
Transcripts					
SP6A		↓	●	↓	↓
HSP70		↑	↑	●	↑
RD29		●	↑	●	↑

● Non-significant change ↑ Increase ↓ Decrease

Figure 7
176x155 mm (x DPI)

1
2
3